Pipeline Damage Prevention Radar

Final Report – Public Version

Prepared for:
U.S. Department of Transportation
Pipeline and Hazardous Materials Safety Administration

In response to:
Contract No: DTP5615T00017
Topic: Damage Prevention

Prepared by:
Todd Pett, Principal Investigator
Phone: (303) 939-6215
Fax: (303) 939-7997
tpett@ball.com

Ball Aerospace & Technologies Corp.
1600 Commerce Street
Boulder, CO 80301
www.ballaerospace.com

February 12, 2018

This research was funded in part under the Department of Transportation, Pipeline and Hazardous Materials Safety Administration's Pipeline Safety Research and Development Program under OTA DTPH5615T000017. The views and conclusions contained in this document are those of the authors and should not be interpreted as representing the official policies, either expressed or implied, of the Pipeline and Hazardous Materials Safety Administration, or the U.S. Government.

Table of Contents

Figures

Tables

1 Introduction

During the Pipeline Damage Prevention Radar (PDPR) project, Ball Aerospace evaluated the use of airborne synthetic aperture radar (SAR) to detect the presence of excavation equipment located on buried pipeline right-of-way areas but obscured from visual detection. SAR naturally penetrates cloud cover, smoke, fog, haze, light precipitation and low light conditions. It has also been shown that SAR can detect erosion and ground subsidence. In addition to these inherent radar benefits, Ball investigated the potential of employing SAR to detect excavation equipment beneath tree cover and surface changes caused by vehicle movement and excavation even when equipment has vacated the area. Armed with this new sensing capability, pipeline operators will have greater flexibility to increase the likelihood of unauthorized excavation threat detection. Such improvements enhance public safety, reduce cost and increase operational efficiency. This research was performed in response to the *Damage Prevention* topic through *Technology Development* in the *Pipeline Safety Research and Development Announcement DTPH5615RA00001* by creating tools that protect new and existing pipelines from excavation damage threats.

PDPR SAR technology leverages decades of development and operational experience realized from Department of Defense (DoD) and NASA funding. Technology advancements now enable SAR to operate within the power constrained, tight confines of small Unpiloted Aerial Vehicles (UAVs), making it straightforward to integrate onto small piloted aircraft currently used for aerial visual inspection patrols.

2 Project Objectives and Scope

The primary objectives of the project were to measure the effectiveness of PDPR at penetrating foliage, detecting excavation equipment beneath the canopy, and measuring ground surface change caused by equipment movement and excavation. In support of these objectives Ball Aerospace proposed to:

- Configure a dual-band SAR system for the PDPR application previously developed for DoD applications and installed on a small, fixed-wing aircraft,
- Identify hardware and software modifications to optimize SAR capabilities for foliage penetration and ground surface change detection applications,
- Perform an initial flight test at the SAR vendor's facility to verify equipment calibration techniques, flight test methods, and to optimize SAR data processing algorithms to enable equipment detection beneath forest canopy, surface change detection, and change measurement superimposed onto optical scene imagery,
- Perform a final flight test in California using aircraft and personnel support contributed by operating partner PG&E. Flights are conducted over the most densely overgrown pipeline rights-of-way identified by PG&E to fully characterize PDPR performance and quantify operational scenario needs for insertion into the commercialization plan.

3 SAR Principles Overview

SAR has been widely used for military and Earth remote sensing applications for more than 30 years. It provides high-resolution, day/night and weather independent imaging capability for a multitude of applications.

An aircraft SAR (Figure 1) operates by transmitting Radio Frequency (RF) pulses from a side-looking antenna (i.e. looking in the direction perpendicular to the direction of flight and downward approximately 45^0 from the horizontal) as the aircraft flies along a straight flight path. Echoes from ground targets are received and processed continuously. As the radar travels along the flight path (azimuth direction) the radar "synthesizes" a long effective antenna aperture by tracking and processing Doppler frequency shifts from received echoes produced by the relative motion between the aircraft and the ground. This "synthetic aperture" enables a small antenna to produce very high resolution of ground features. Resolution in the orthogonal range (or elevation) dimension is enhanced through the process of pulse compression commonly employed by conventional radars. By employing both antenna "beam sharpening" signal processing techniques, SAR produces very high resolution of ground targets.

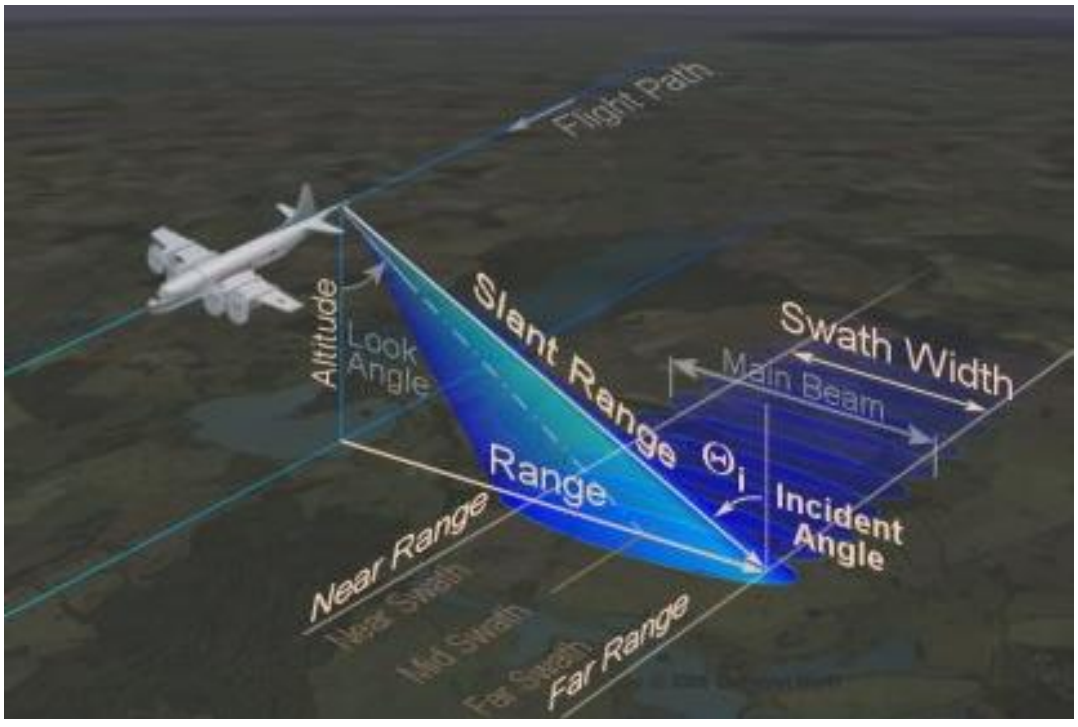

Figure 1. Airborne SAR imaging configuration. The side-looking antenna illuminates a swath of Earth as the aircraft travels along a straight flight path. Width of the ground swath is determined by the antenna's main beam beamwidth and flight altitude. The SAR continuously receives echoes from the transmit pulses and processes them into high resolution images.

Each point in the ground swath scatters a small portion of the incident pulse back toward the radar creating a small signal contribution with a unique amplitude and phase. Backscatter signals from many points are combined coherently to produce a single signal magnitude for each pixel in the SAR image. A typical image will look like the example in gray scale shown in Figure 2. The intensity of each image pixel varies in direct relation to the measured echo signal amplitude i.e. lighter gray shades indicate increasing radar echo reflectivity.

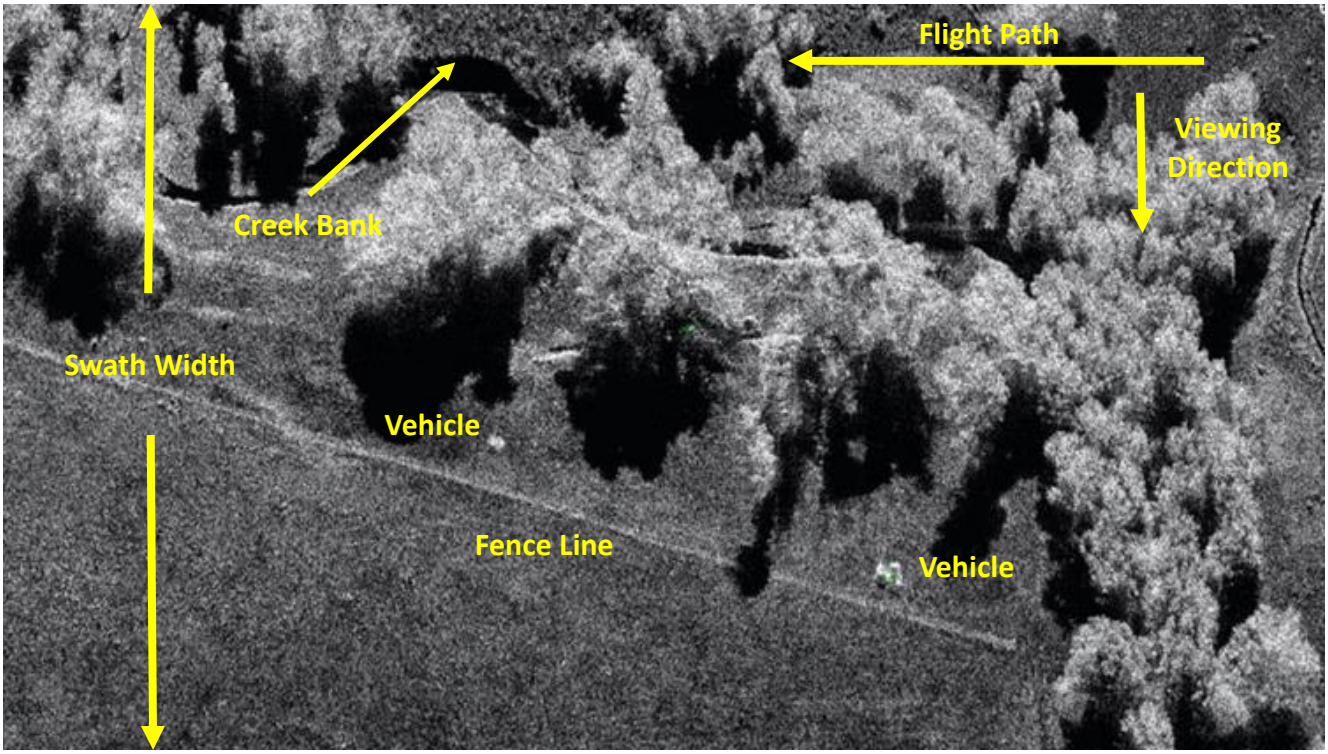

Figure 2. SAR image of a creek surrounded by trees. The aircraft flight path is from right to left and the antenna is looking from the top of the image downward. In this example, the tree canopy is highly reflective so appears in the lightest shade of gray. The darkest patches are shadows produced by trees and a steep downward facing creek bank. A fence line and two vehicles are also clearly visible due to the high reflectivity of metallic objects.

The SAR processing technique improves the target resolving capability along the direction of flight which is a shortcoming of conventional radar. As demonstrated in DoD applications (looking for hidden, mechanized weaponry), side-looking SAR processes multiple echoes for enhanced resolution and target identification. SAR is especially well suited for identifying metallic items, *e.g.* unauthorized equipment in right-of-way areas. The strength of reflections from metallic objects combines with penetration through visual obscurations yielding more reliable threat-detection than visual inspection, even with optical enhancements. Figure 3 depicts pipeline aerial survey operation using SAR. This improved resolution capability combined with the ability to see through foliage and adverse weather makes SAR an ideal choice for this damage prevention application.

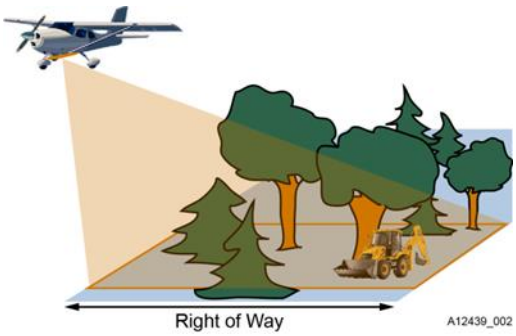

Figure 3. Side-looking SAR identifies excavation threats for damage prevention even where visual inspection and advanced optical imaging techniques fail.

Change detection (CD) with SAR involves a pair of images, of the same area that were collected under the same system setting and geometry conditions but at different times. To identify changes, different methods are commonly applied and differ with respect to the parameters that are used to highlight changes. Since SAR data contains amplitude and phase information, both parameters can be used as indicators of change. Incoherent CD, also known as amplitude or magnitude CD (MCD), identifies changes by comparing estimates of the mean backscatter power taken from the repeat pass image pair. The coherent change detection (CCD) technique includes the phase coherence of a SAR image pair to quantify changes in both the amplitude and phase of the image pixels. Because phase information is included in the process, the CCD technique is typically more sensitive to change than MCD. However, the increased sensitivity can also increase the susceptibility to false detections.

CCD is widely employed to enhance the detection of objects and surface change. CCD exploits the sensitivity of the SAR image speckle pattern and image phase determined by the structure of the scene scattering mechanisms to detect subtle scene changes that may occur in the time interval between a repeat pass imaging collection. Small perturbations caused by the compaction or displacement of soil (e.g. from vehicle traffic), vegetation, or rock (e.g. from excavation or erosion) will induce a measurable change. Figure 4 illustrates the capability of CCD. In this example, the CCD extracts change produced by vehicle tracks, soil disturbance and movement of vehicles. The sensitivity of the CCD technique allows the identification of potential problem areas where the ground is shifting or eroding. In situations of natural disaster such as flood or earthquake, this information will prove valuable in verifying the integrity and continued safe operation of the pipeline.

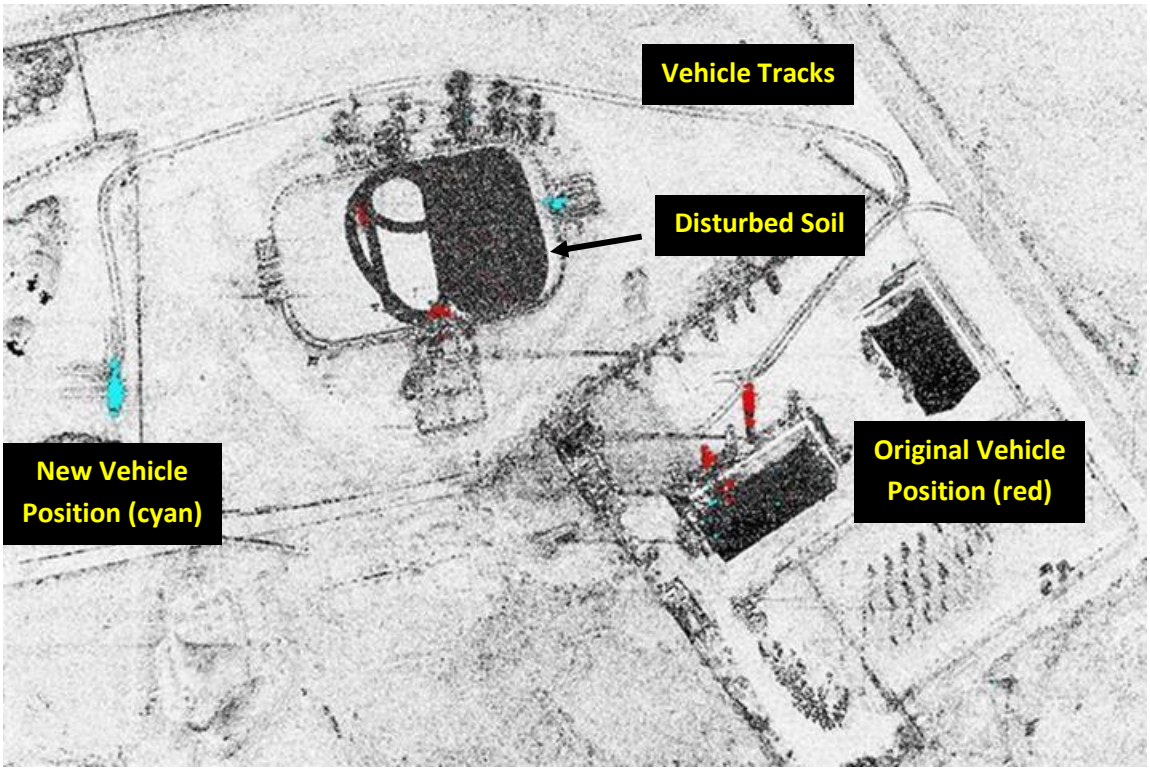

Figure 4. In this SAR CCD image, red pixels indicate removal of an object from the scene, while cyan color indicates arrival of an object to the scene. In this example, a vehicle has moved from near the center of the image (red position) to the left of the image (blue position). By effective processing of phase information, changes like vehicle tracks, not visible to the eye, can be detected. Tire tracks and soil disturbance (dark areas) are readily visible.

4 Airborne SAR System

The airborne SAR system produced by IMSAR of Springville, Utah was selected to support this project and to complement the SAR image processing expertise at Ball Aerospace. IMSAR's family of *NanoSAR* products have logged over 10,000 flight hours on a variety of airframes ranging from Twin Otter and single engine Cessna aircraft to Unpiloted Aerial Vehicles (UAVs) as small as the catapult launched Shadow UAV built by AAI Corporation (Figure 5).

Figure 5. The Shadow UAV primarily used by the US Army weighs approximately 170 kg and is designed for reconnaissance, surveillance, target acquisition and battle damage assessment.

The primary components of *NanoSAR* are the small, lightweight transceiver, antenna, *Viper* downlink and *LISA-3D* image processing systems. With the appropriate antenna attached, the *NanoSAR* system can operate over specific bandwidths within the UHF (300 MHz – 3 GHz), X (8 - 12 GHz) and Ku (13 – 18 GHz) frequency bands or over a wider bandwidth when operating in the Ultra-Wideband (UWB) mode. Figure 6 summarizes the key performance attributes of the *NanoSAR system*.

Figure 6. IMSAR's *NanoSAR* radar is lightweight, compact and offers multi-band operational capability.

The two highest frequency band radars (i.e. X and Ku-band) are self-contained in pods attached beneath the wing of IMSAR's Cessna 172 aircraft. The UWB radar electronics reside inside the plane and the UWB antenna consists of an array of Log Periodic (LP) antennas attached to the outside of the airframe. An array of antennas increases the signal-to-noise ratio (SNR) and provides the added capability to suppress sources of radio frequency interference (RFI) that may be operating in the SAR band and corrupting imagery. The airframe integrated antenna configurations are shown in Figure 7.

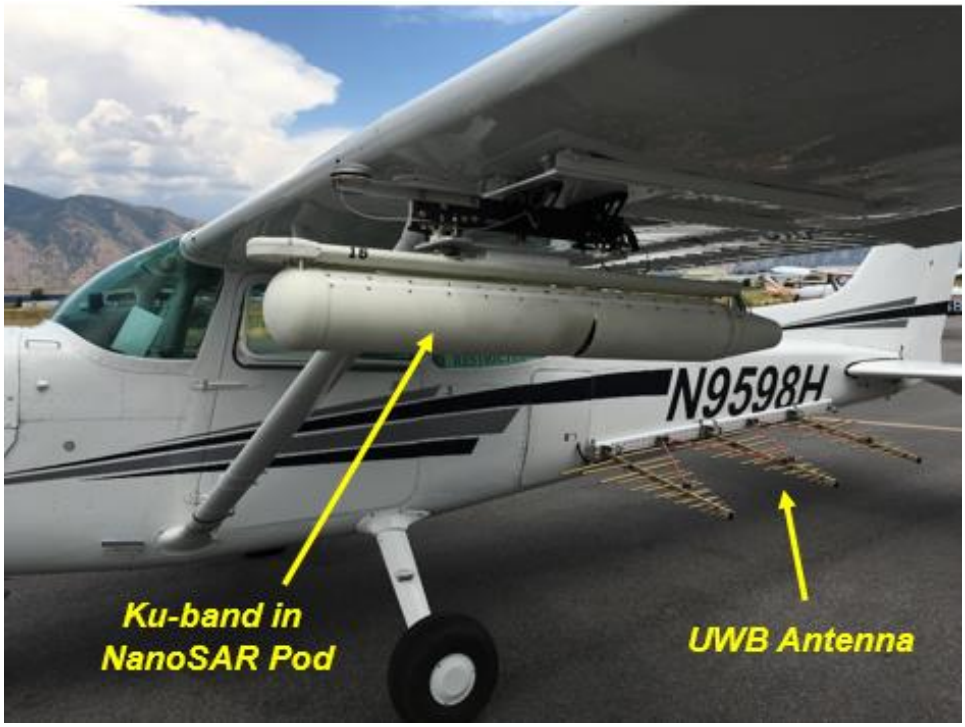

Figure 7. Ku-band Pod and UWB Antenna Array

5 Field Testing

The Springville, Utah area-based testing of the PDPR system focused on demonstrating the capability of SAR to detect excavation equipment beneath foliage and surface changes from vehicle incursion and excavation. Initial flight tests were performed in June 2016. The flight tests were repeated in July/August of 2017. Various observations with staged ground truth targets provide sufficient data to qualitatively and quantitatively assess performance and operational potential. The testing improves our understanding of the PDPR's ability to detect the location of pipeline damage threats for a variety of different targets. Additional "day-in-the-life" measurements were included in the July 2017 collections to test the system capability in a more realistic operational scenario.

Key objectives of the testing included the following:

1. Obtain clean, repeatable SAR measurements and co-registered, high resolution optical imagery.
2. Obtain data that can be demonstrated as a "day in the life" of the SAR i.e. overfly an existing buried pipeline right-of-way. Detect threats and measure surface changes.
3. Understand system sensitivities:
    a. What sizes of targets are detectable beneath foliage and in the open?
    b. How well can tire tracks be detected using the CCD processing?
        i. Can tire tracks be detected after 2 to 3 days?
4. Quantify the system capability in both rural and urban environments
5. Understand the system detection / false alarm rate in open areas and under foliage
    a. Given a target of a certain size, what is the detection and false alarm rate?

The following sections detail the two types of tests performed: Staged tests, and day-in-the-life tests. Staged tests provide analysis of types of targets detectable both in the open and under foliage. The day-in-the-life test provides an example of how the system might work in an operational environment.

5.1 Staged Tests

Staged testing is accomplished by performing pre-defined SAR imaging data collections over urban and rural areas with targets staged both in the open and under foliage.

Each day starts and ends with baseline flights with no staged targets. The initial baseline flight is flown twice to ensure repeatability of the measurements. After the baseline flights are completed, targets are staged in pre-defined areas. The areas are photographed and locations of staged targets are recorded along with the staging time and GPS coordinates. Other pertinent information is also recorded including where vehicles had been driven, and any other movements that might have disturbed the soil. The SAR system images the area at least once. Subsequent passes are performed as determined by the test conductor. After the data quality is deemed acceptable, the targets are moved to new locations and the flights repeated.

Four areas near Springville provided a range of environments for staged data collection:

1. Spanish Fork (urban terrain)
2. Provo Cemetery (rural terrain)
3. Lakeshore (rural terrain near Utah Lake)
4. Birdseye (rural terrain in Spanish Fork Canyon).

For each of the staged areas, a flight path was determined that includes the area of interest and surrounding locations. Flight paths for the staged areas are shown in Figures 8 and 9.

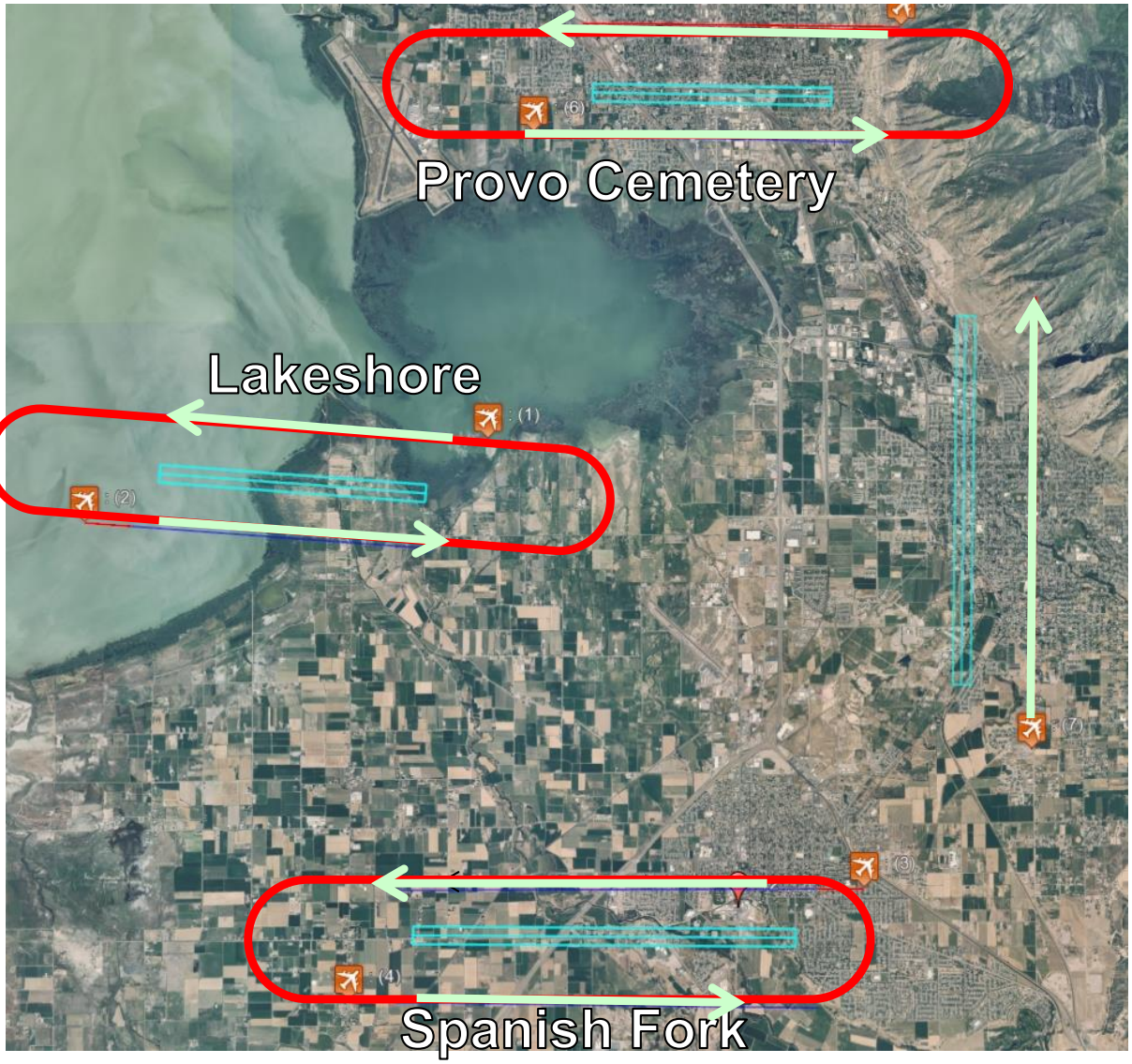

Figure 8. Flight paths for PDPR testing in Utah Valley.

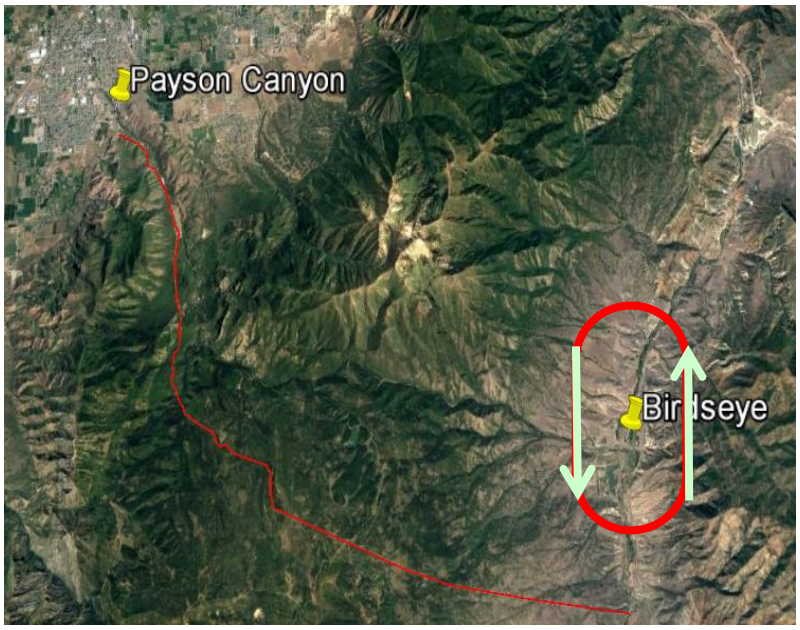

Figure 9. Flight paths for PDPR testing up Payson Canyon and in Birdseye

For each of the staged locations, several types of targets were placed both beneath foliage and in the open. The following items were staged:

1. Backhoe
2. Pickup
3. Wheelbarrow & shovels
4. Large corner reflector (CR)
5. Small CRs
6. SUV, small pickup or automobile

5.2 Day-in-the-life Testing

The PDPR system was flown over an actual pipeline right-of-way near Payson Canyon (Figure 9). The day-in-the-life test was performed twice, with two days between collections. Data analysis was performed on the two datasets to identify any changes occurring between the two. No targets were staged during the day-in-the-life test.

5.3 Sensor Configurations

IMSAR has developed several sensors that cover various parts of the electromagnetic spectrum: a Ku-band SAR system, an X-band SAR system, a UWB system that operates at Ultra High Frequency (UHF – 300 MHz to 3 GHz), and an optical camera system. Due to Federal Communications Commission (FCC) licensing restrictions, only a portion of the full UWB band can be utilized in most areas of the United States. Since some areas are more restricted than

others, we evaluated two UWB sub-bands, one covering 420 to 960 MHz, which represents the portion of the full UWB band authorized for use in Utah, and 750 to 960 MHz which represents the portion authorized in Sacramento, CA where we had originally planned to fly the PDPR for the second round of tests. To assess various sensors' applicability to pipeline damage prevention, we tested three sensor configurations in 2016 and 2017 that utilized the various sensors and approved bands.

For each configuration, ground resolution in the range (elevation) direction is directly proportional to bandwidth of the transmitted pulses. For the UWB sensor, the wider bandwidth (540 MHz used in Utah) produced the highest resolution. Even though we did not fly in Sacramento, we still generated results using the reduced bandwidth to assess performance under the limited bandwidth condition. The resolution in the along-track (azimuth or synthetic aperture) direction is independent of bandwidth and only depends upon the available beam width extent of the antenna. Bandwidth affects only the SNR in the along-track direction, with increased bandwidths providing higher sensitivity.

5.4 Summary of the June 6 - 9, 2016 Field Test

During the June 2016 field test, we performed flights over the Utah valley sites (Lakeshore, Spanish Fork, and Provo Cemetery) on June 6th and June 7th and over Birdseye on June 8th and 9th. On June 6th and 8th, the Ku-band sensor and narrow band UWB (210 MHz) bandwidth were utilized. On June 8th, thin air and turbulence over the Birdseye site made it difficult to maintain the required attitude so this configuration was re-flown on June 9th. The X-band sensor with the wider 540 MHz UWB bandwidth was flown on June 7th over the Utah Valley sites and on the 9th over Birdseye.

Co-registration of optical and SAR images adds the visible terrain context critical to accurate determination of threat assessments. A breadboard version of an EO sensor (5 Mpixel camera) mounted beneath a wing was flown with the radars during the June 6 - 9th test flights. During this first test, the camera was not gimballed and did not adequately co-locate optically with the SAR images. Regardless, this preliminary configuration provided useful information on the value of multi-spectral overlay of imagery. Several system settings for the June 6 - 9, 2016 field test are shown in Table 1.

Table 1. SAR System Settings used during the June 6th–June 9th 2016 field test

June 6 – 9, 2016 (Ku, X, UWB-Wide, UWB-Narrow)				
Sensor	**Altitude (AGL)**	**Resolution**	**Swath Width**	**Dates Flown**
KU	3000 ft	3.9 inches	980 ft	6/6/2016, 6/8/2016, 6/9/2016
X	3000 ft	5.8 inches	730 ft	6/7/2016, 6/9/2016
UWB-Wide	3000 ft	11.5 inches	1415 ft	6/7/2016, 6/9/2016
UWB-Narrow	3000 ft	2.3 ft	5920 ft	6/6/2016, 6/8/2016, 6/9/2016

During the Utah valley tests, we stationed a target staging group at each of the three sites. Within each site, three targets were staged in the open and under foliage. The objects were observed by the SAR system from two directions, one of which looked through the foliage, and the other viewed the targets mostly in the open. After imaging the area, the staging group rotated to the next Utah valley test site and staged their targets in the same locations used by the prior staging group. This test allowed us to observe targets both in the open, and under several types of foliage. Two initial baselines were performed in which no targets were present. After each of the staging groups rotated through each site, a final baseline was performed. The test sequences for the Utah valley tests on June 6th and 7th are shown in Table 2.

Table 2. Test sequence for Utah valley tests on June 6th, 2016 (Ku and UWB-Narrow) and June 7th, 2016 (X and UWB-Wide).

	Targets	Baseline (2X)	Test 1	Test 2	Test 3	Baseline
Group 1	Backhoe, SUV, Wheelbarrow	absent	Lakeshore	Spanish Fork	Provo Cemetery	absent
Group 2	Pickup, Small CRs, Large CRs	absent	Spanish Fork	Provo Cemetery	Lakeshore	absent
Group 3	Rental Car, Shovels, Raked Soil	absent	Provo Cemetery	Lakeshore	Spanish Fork	absent

Examples of X-band SAR imagery collected over the Lakeshore foliage covered test area are shown in Figure 10. Representative examples of Ku and UWB images are shown in subsequent sections. In the top SAR image of Figure 11, the faint outlines of the road boundaries are evident. Successful detections of staged targets (e.g. backhoe or SUV) are indicated by the bright dots at the center of each yellow circle. The bottom image depicts a CCD result for the same test area. Due to the high coherence of the road boundaries between master and slave images the difference is negligible so no change appears in the CCD image. However, the foliage decreases the coherence and produces multiple false indications of change which are indicated by the red and cyan spots. The true locations of the objects are within the yellow circles.

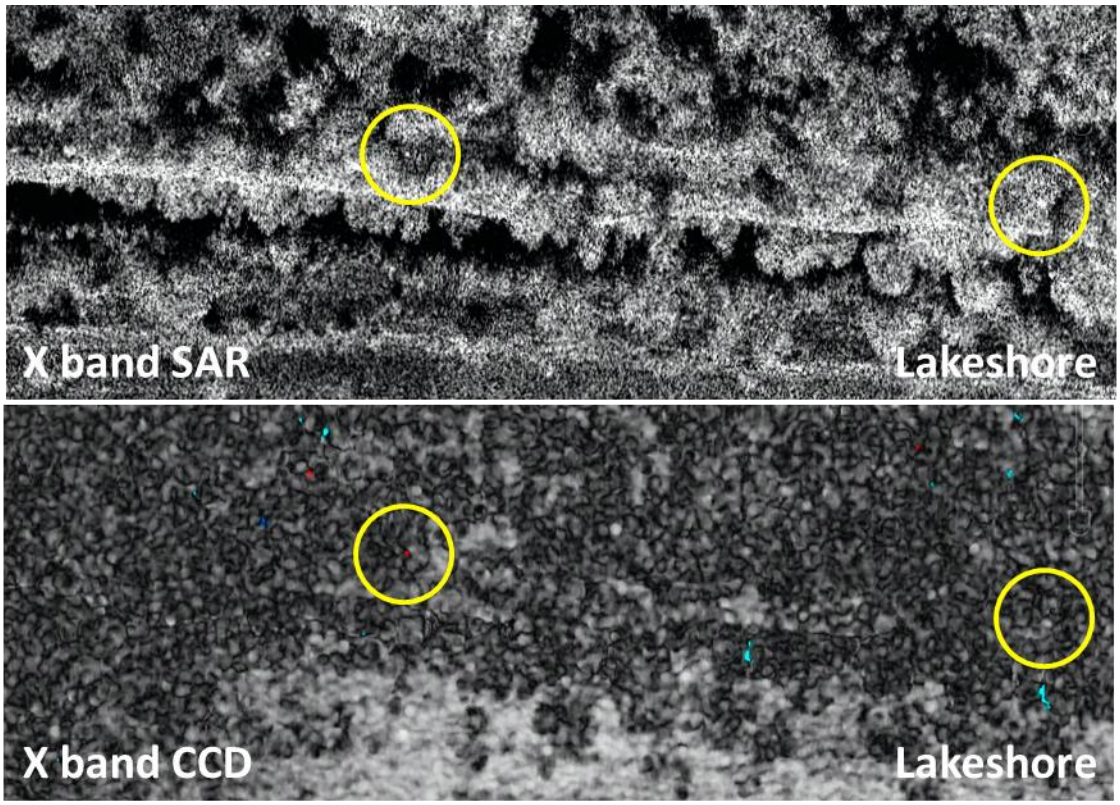

Figure 10. X band SAR image (top) and CCD results (bottom) showing detections of targets (yellow circles) in the Lakeshore test area on 6/7/2016. The SAR image appears clear and targets can be detected visually, but low coherence in the CCD caused by foliage hinders the detection of all targets. SAR transmission is from the bottom facing up into the image.

Figure 11 depicts a sample of results from the Spanish Fork test area. Spanish Fork urban test site provided increased density of residences and infrastructure, e.g. streets and power lines, to assess the capability of object detection and CCD. The SAR image clearly shows the outlines of structures. The parallel lines near the bottom are radar image representations of power lines. The yellow circles indicate the positions of two staged targets. There is "streaking" in the image that is caused by RFI. The lower CCD image shows the change produced by placement of staged objects at the positions highlighted by the yellow circles (same positions as in the SAR image). However, due to image registration errors, the coherence is low resulting in a number of false change detections indicated by the numerous other red and cyan areas.

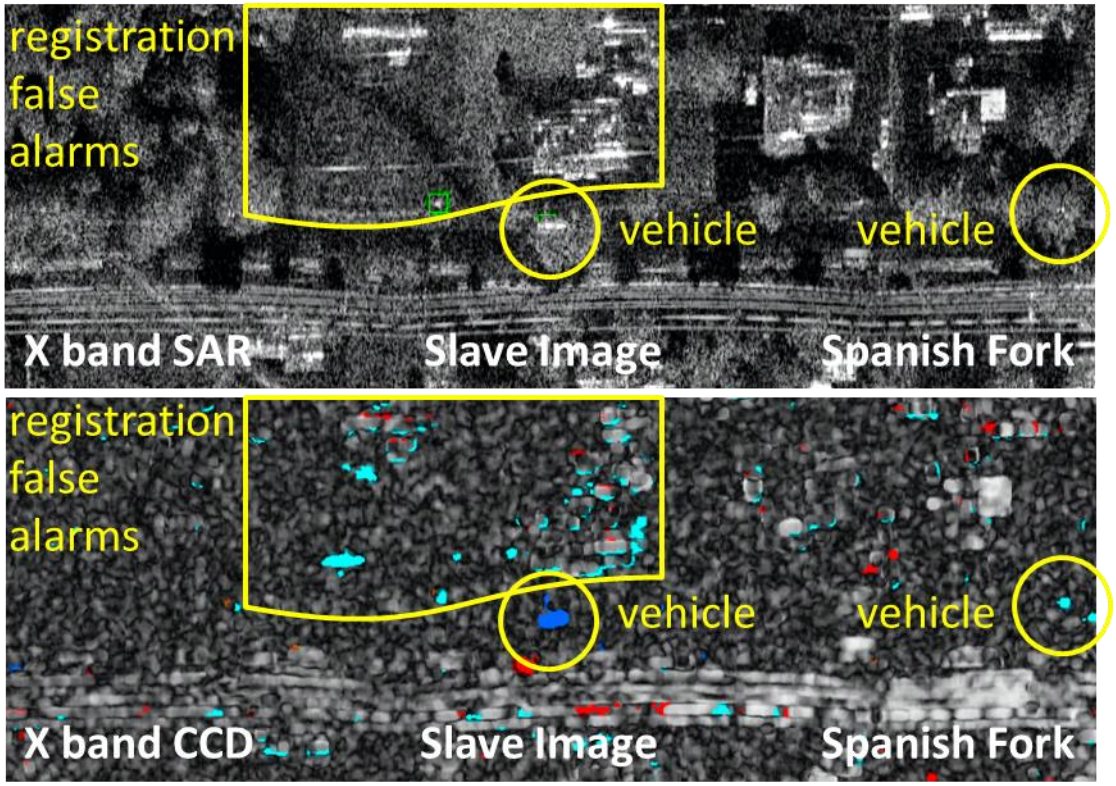

Figure 11. X band SAR (top) and CCD (bottom) results showing detections of targets (yellow circles) in the Spanish Fork test area on 6/7/2016. The SAR image appears clear but there are indications of RFI and streaking. The targets were detected in the CCD but mis-registration and RFI caused a large number of false alarms and low coherence in the CCD image. SAR transmission is from the bottom facing up into the image.

Figure 12 show results for objects staged inside the Provo cemetery which we considered representative of a rural environment. Once again the staged objects are visible in the SAR image. The CCD image clearly shows object movement between the initial overflight and repeat pass data collection. In this example image mis-registration was less of an issue so there were fewer false detection indications.

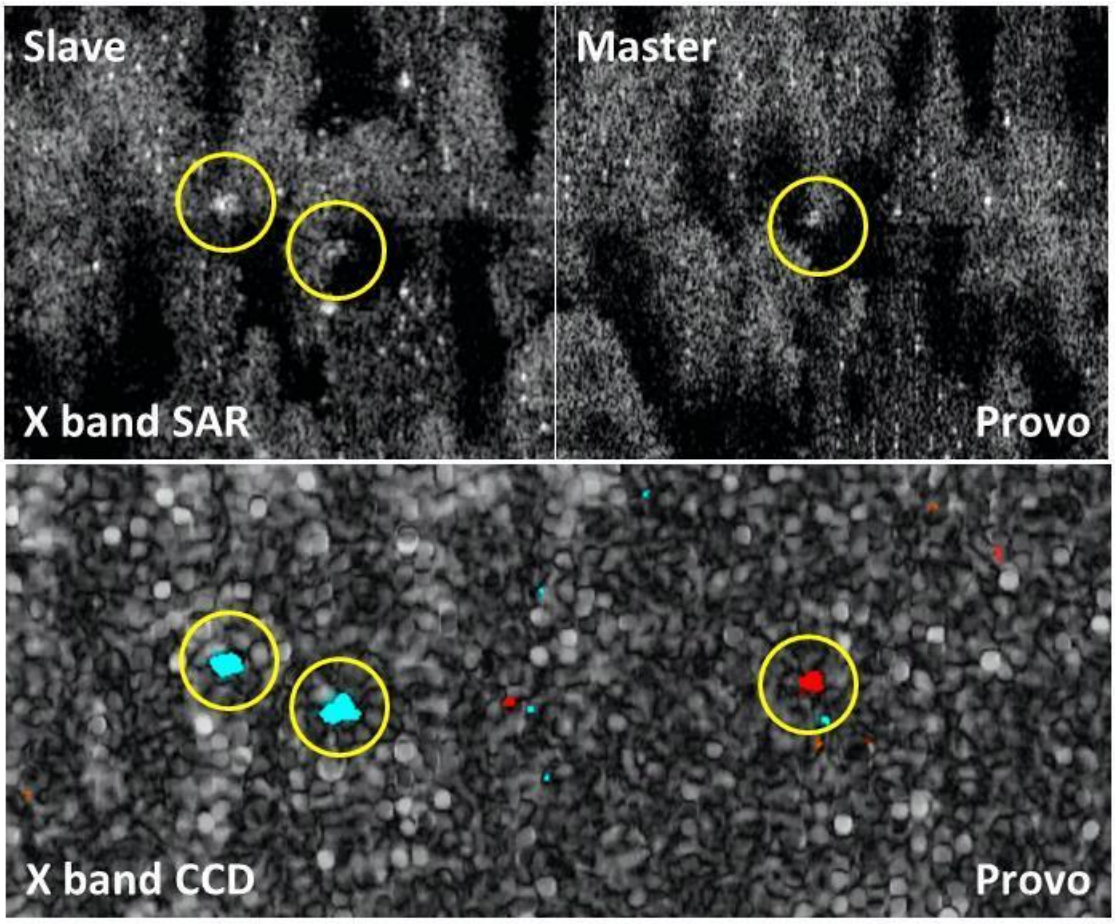

Figure 12. X band SAR and CCD results showing target detections (yellow circles) in the Provo Cemetery test area on 6/7/2016. The slave image is slightly blurred causing lower coherence and a few false alarms along the edges of trees. Large targets are easily detected. SAR transmission is from the top of the image facing down.

The Birdseye test site was the most remote and rural environment that was tested. At this location various targets were staged as shown in Table 3. During each test, the targets were moved to new positions or rotated amongst positions already in use. This test was originally intended to be a blind test to determine if the image analyst could identify targets without prior knowledge of their locations. However, anomalies resulting caused by image mis-registration, blurring, and INS data drop-outs required us to re-evaluate the objectives for testing on that day. The decision was made to abandon the blind test idea and focus on data collection, characterization of anomalies and development of an anomaly mitigation plan.

Table 3. Test sequence for the Birdseye Tests on June 7th, 2016 (Ku and UWB-Narrow) and June 8th, 2016 (X and UWB-Wide, Ku and UWB-Narrow repeat)

	Targets	Baseline (2x)	Test 4	Test 5	Test 6	Baseline
Stager 1	Small CR, Shovels	absent	In Position	Change Positions	Rotate Positions	absent
Stager 2	Ranger (ATV), Small CR, Shovel	absent	In Position	Change Positions	Rotate Positions	absent
Stager 3	Backhoe Small CR	- Backhoe in Position - Small CR Absent	Change Positions	Change Positions	Change Positions	- Backhoe in Position - Small CR Absent
Stager 4	Large CR, Small CR, Wheelbarrow	Absent	In Position	Rotate Positions	Rotate Positions	absent

A sample of the SAR data collection results from Birdseye are shown in Figure 13. During this test we were able to collect data at all three frequency bands (UWB, X and Ku) for direct comparison. The Ku-band system produces the best resolution. There is slightly less blurring of the trees and a less grainy appearance of the terrain in the open areas than in the X-band image. The resolution degrades with decreasing frequency as evident from the UWB SAR and CCD images. The tree images are blurrier and the open terrain features are grainier and less pronounced. Target locations are indicated by the yellow circles.

While the lower frequency range is better at penetrating foliage it is also more susceptible to reflections from long, linear metallic features. Metal fences and pipes that were barely noticeable in the higher frequency images are quite pronounced in the UWB image. Also, there are ghost images on either side of main image from each linear feature.

CCD performance was relatively good at this site as indicated by the color coding of object position changes. There was still some degradation (coherence loss) due to image mis-registration and blurring.

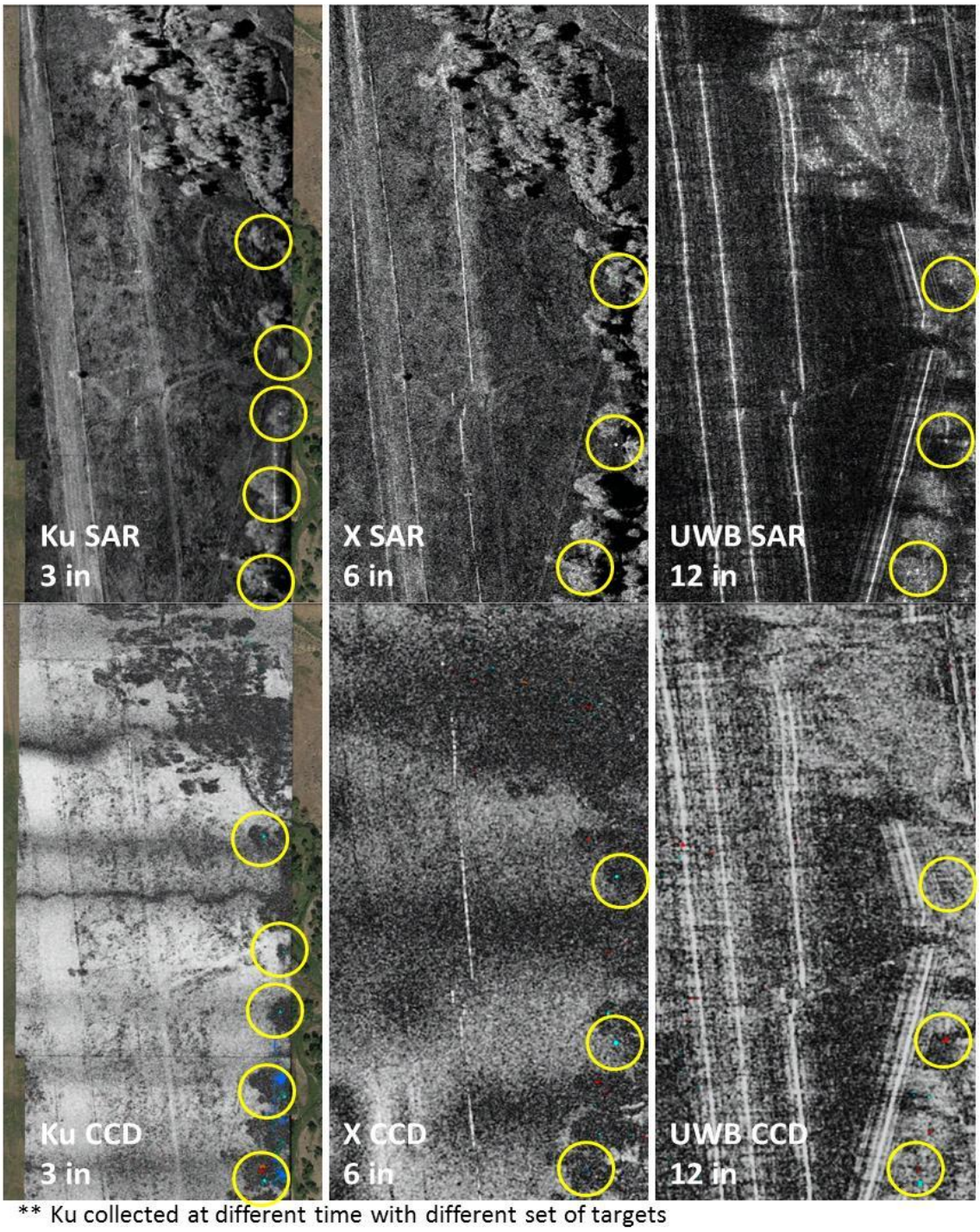

Figure 13. Ku, X and UWB band SAR and CCD images showing detections of targets (yellow circles) in the Birdseye test area on 6/9/2016. Problems with image registration and blur caused areas of low coherence. The UWB images also show secondary reflections near long linear features. Based on the radar frequency, each sensor provides a different spatial resolution. SAR transmission is from the left side of the image facing right.

5.5 Summary of July 11 – 13 and August 24, 2017 Field Tests

Due to data anomalies experienced during the June 2016 field tests and a desire for improved performance, we re-flew the Utah sites in July and August 2017 with the following changes to the initial system configuration and the test plan:

1. The wing-mounted camera was upgraded to 18 Mpixel resolution and installed onto a gimbal to provide optical imagery co-boresighted with the SAR data.
2. A new 3-element LP antenna array configuration was used for the UWB to help reject RFI, improve SNR and reduce ghosting/scratching/blurring in images collected during the June 2016 tests. The June 2016 testing was performed with a single LP antenna element.
3. Results from the June 2016 tests showed that the Ku-band antenna gimbal wasn't pointing the antenna as accurately as required. This problem was mitigated through a software upgrade prior to the 2017 tests.
4. The performance of the data downlink system was improved reducing the incidence of data loss that was experienced during the initial June 2016 test.
5. The June 2016 testing revealed errors in the position data reported by the INS causing image blurring and registration errors between master (baseline) and slave images. Mis-registration between images also increases the incidence of false change detection. A software upgrade was designed and installed to mitigate this effect.
6. Results from the June 2016 tests showed that the Ku-band sensor produced higher resolution and would perform better than the X-band system, so the decision was made to remove the X-band sensor from the test plan and focus solely on a dual band system i.e. UWB and Ku-band.
7. The UWB-Wide bandwidth was used. UWB-Narrow narrowband performance was simulated by reducing the bandwidth during post-processing.
8. Targets were staged both in the open and in concealed locations.
9. Targets were no longer staged in the same location as previous targets. This allows us to better differentiate when a target had moved.
10. Only one set of targets were used in each area (first in the open and then concealed), rather than rotating all targets through all areas. The backhoe and SUV were imaged in Lakeshore, and the Pickup and corner reflectors were imaged in Spanish Fork and Provo Cemetery.
11. New data processing routines at IMSAR including INS filtering and updated image registration libraries provided improved data quality.

We learned after the test that the EO sensor experienced an anomaly on July 12, 2017 resulting in the loss of optical image data over the Utah valley on that day. An additional test day was scheduled for August 24, 2017 to re-fly the Utah valley and collect optical images with the SAR data that were absent during the previous attempt. The configuration of the sensors for these repeat data collects are shown in Table 4.

Table 4. System Settings used during the July 11th–July 13th, 2017 and August 24th, 2017 Field Tests

July 11 – 13 and August 24, 2017 (Ku, UWB, EO)				
Sensor	**Altitude**	**Resolution**	**Swath Width**	**Dates Flown**
KU	3000 ft	3.9 inches	980 ft	7/11/2017 - 7/13/2017, 8/24/2017
UWB	3000 ft	11.5 inches	1415 ft	7/11/2017 - 7/13/2017, 8/24/2017

The test sequence for the Utah valley testing on July 12th and August 24th are shown in Table 5. For each test, the targets were stationed in open areas and then in concealed areas. Again the areas were baselined without targets prior to and after the staged testing. At Lakeshore, the backhoe and SUV were positioned in various concealed areas and in various orientations to provide different views of the backhoe. In all configurations, the targets were visible or at least partially visible from one of the two observation directions.

Table 5. Test sequence for Utah valley tests on July 12th, 2017 (Ku and UWB-Wide) and August 24th, 2017 (Ku and UWB-Wide).

	Targets	**Baseline (2X)**	**Test 1**	**Test 2**	**Test 3**	**Baseline**
Group 1	Backhoe, SUV, Wheelbarrow	absent	Lakeshore Open, Lakeshore Concealed*			absent
Group 2	Pickup, Small CRs, Large CRs	absent		Spanish Fork Open, Spanish Fork Concealed	Provo Cemetery Open, Provo Cemetery Concealed	absent

* Multiple concealed locations were staged for the Lakeshore area

The test sequence for the Day-in the life testing through Payson Canyon and Staged testing in Birdseye testing on July 11th and July 13th, 2017 is shown in Table 6. All targets at Birdseye were staged first in the open and then in concealed locations. On July 13th, multiple concealed locations were imaged.

Table 6. Test sequence for Birdseye tests on July 11th, 2017 (Ku and UWB-Wide) and July 13th, 2017 (Ku and UWB-Wide).

	Targets	Day in the life (Payson Canyon)	Baseline (2X) (Birdseye)	Test 1 (Birdseye)	Test 2 (Birdseye)	Baseline (Birdseye)
Stager 1	Small CR	absent	absent	Staged in Open	Staged Concealed*	absent
Stager 2	Wheelbarrow, Large CR	absent	absent	Staged in Open	Staged Concealed*	absent
Stager 3	Ranger, Large CR	absent	absent	Staged in Open	Staged Concealed*	absent
Stager 4	Backhoe	absent	In position	Staged in Open	Staged Concealed*	In Position
Stager 5	Pickup / Tire Tracks	absent	In position	Staged in Open	Tire Tracks Created Staged in Open	In Position

* Multiple concealed locations were staged for the Birdseye area on 7/13/2017

As mentioned, a key improvement for the 2017 data collections was the incorporation of a co-boresighted high resolution optical camera. Having the optical imagery along with the SAR data helps provide context and the ability to characterize a specific change. Please note that shadows in the optical image indicate the direction of solar illumination, while shadows in the SAR data indicate the direct of radar illumination. Optical camera and SAR shadows therefore often occur in different locations as can be seen in Figure 14.

Figure 14 shows a 24 August collect against targets in the open at the Lakeshore test location. The targets included a backhoe, a dark SUV, and a wheel barrow. In Figure 14, the backhoe and SUV can be seen to be collected from the side and the wheel barrow from the front. Each target was detected in the respective UWB and Ku SAR image, but as seen in Figure 15, the wheel barrow was not identified as a change in the Ku CCD image at the current threshold settings. This is likely due to the small size and rounded corners of the wheel barrow. Tire tracks occurring after the collection of the master SAR image can also be seen in the Ku CCD image.

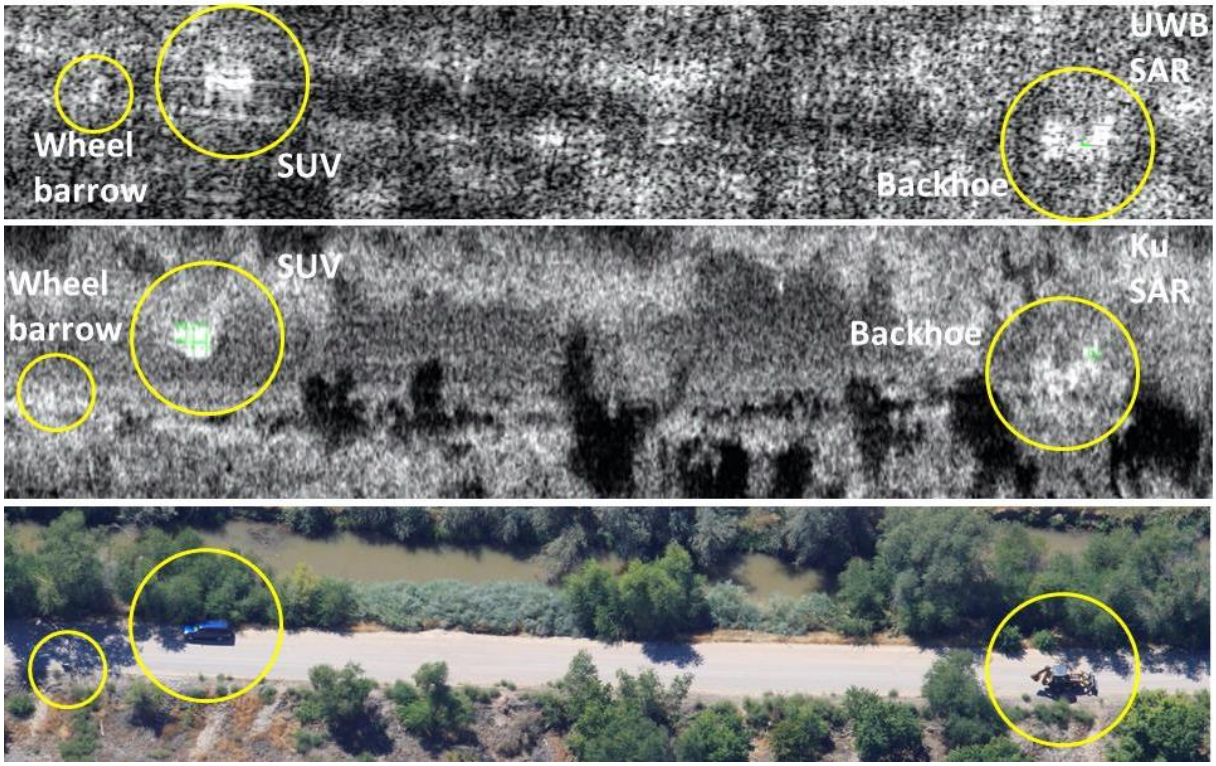

Figure 14. Ku and UWB SAR images showing detection of the backhoe, SUV and wheel barrow targets in open positions. The small wheel barrow can be visually observed in the Ku data but was not detected by the magnitude CD algorithm at the current threshold settings. SAR transmission is from the bottom facing up into the image.

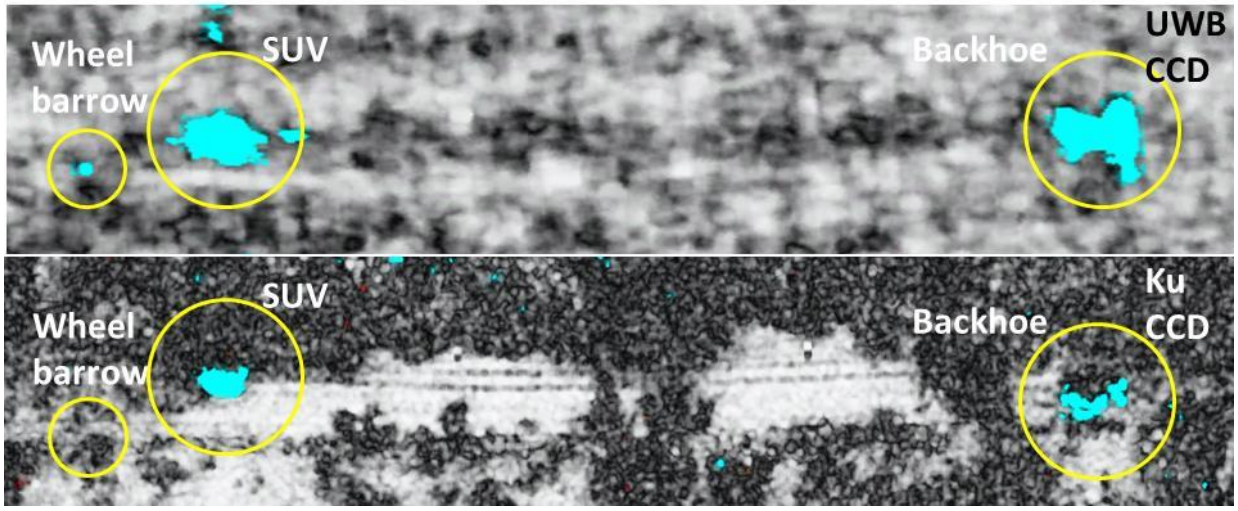

Figure 15. CCD images where the blue color indicates that an object was new to the scene. Tire tracks occurring after the collection of the master image can also be seen in the Ku CCD image. SAR transmission is from the bottom facing up into the image.

Figure 16 shows the same 24 August collection geometry but from the opposite side as indicated by EO and Ku SAR shadows in similar locations. The backhoe and SUV are again easily detected but the wheel barrow was not as it was completely blocked by a large set of trees. Tire tracks are again visible in the Ku CCD image shown in Figure 17. A few false alarms associated with tree movement can also be observed.

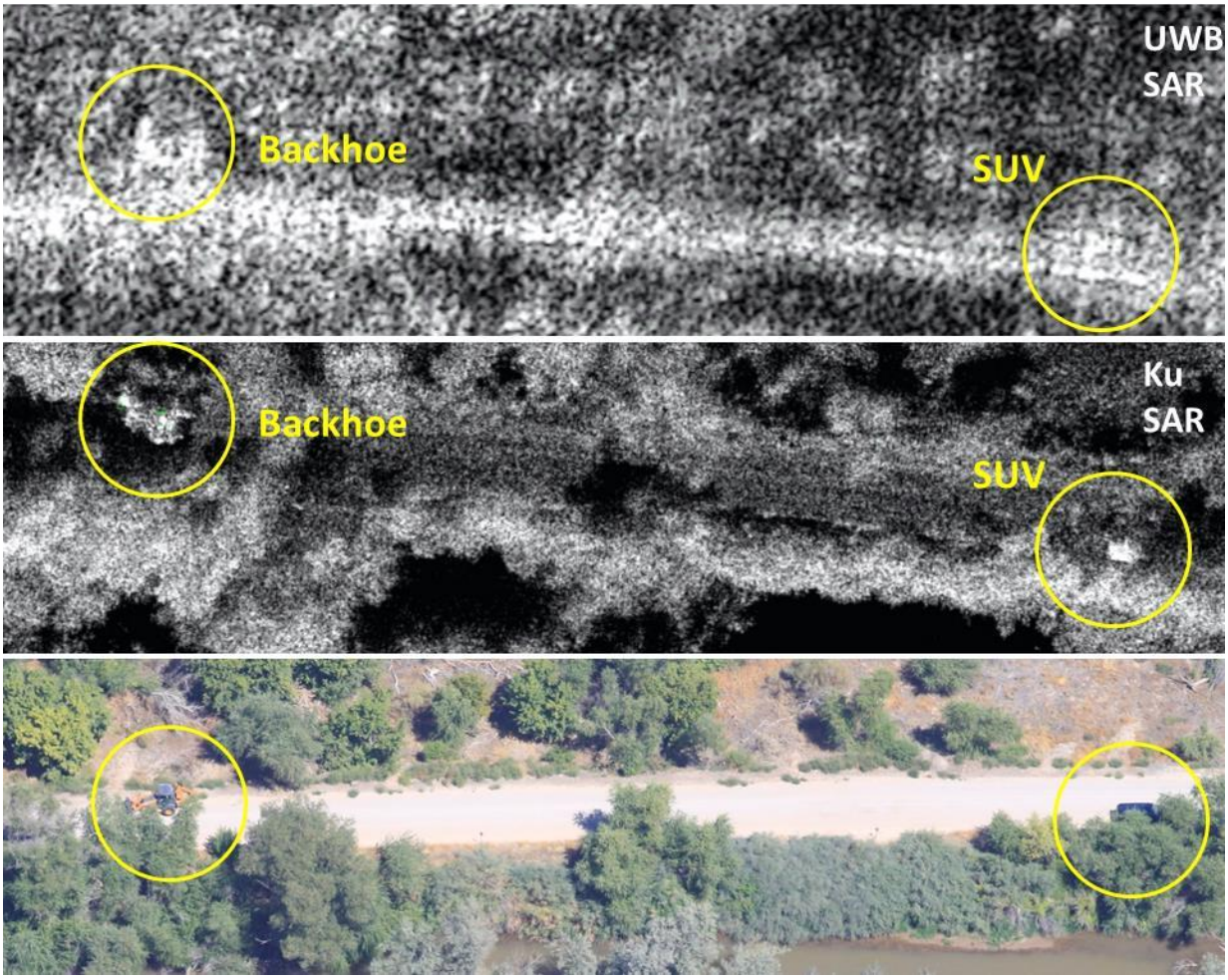

Figure 16. Ku and UWB SAR images showing detection of Backhoe and SUV targets in partially vegetation obscured locations. The wheel barrow is completely vegetation obscured and not detected. SAR transmission is from the bottom facing up into the image.

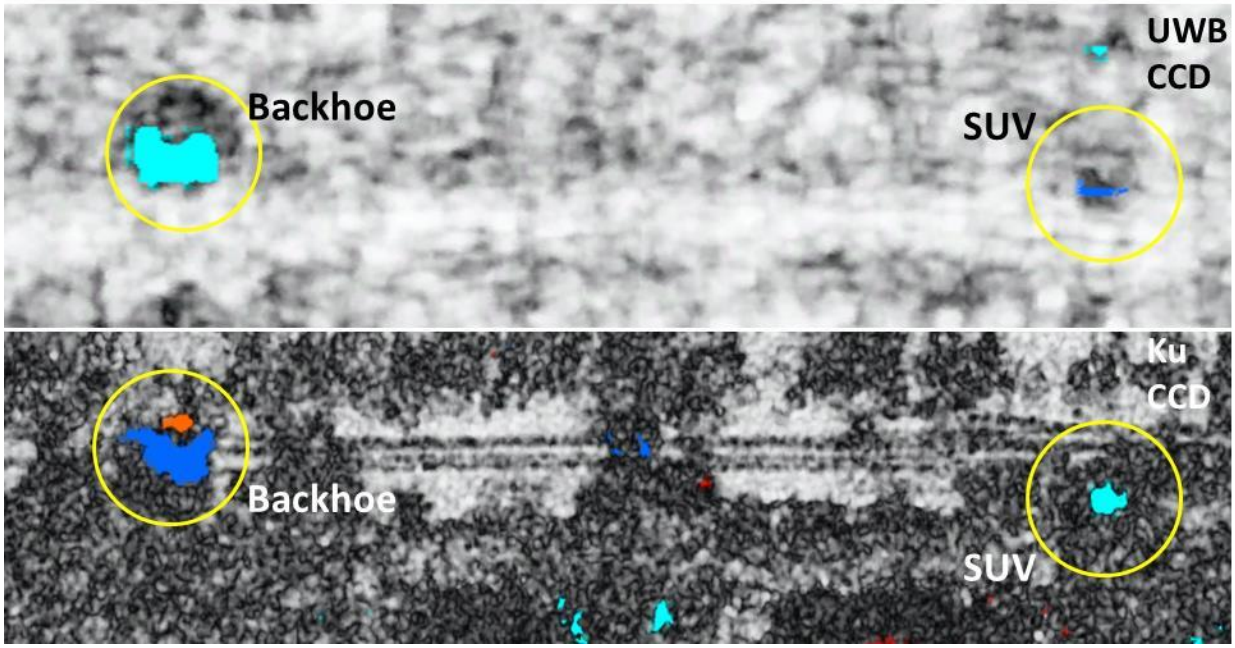

Figure 17. CCD results showing target detections and vehicle tracks. SAR transmission is from the bottom facing up into the image.

Figures 18 and 19 show a different 24 August collection geometry where the backhoe and SUV are largely obscured by foliage from one direction. In Figure 18 the backhoe can be seen to be in the open and easily detected, while the SUV is largely obscured and difficult to detect. As discussed previously, targets in the open are easily detected in both the Ku and UWB. In contrast, detection performance of predominately obscured targets varies based upon the size of the object and the strength of the returned radar signal. In Figure 18, the SUV is only weakly detected, while in Figure 19, the backhoe Ku detection is smaller but easily seen. The backhoe was not detected in the figure 19 UWB image. The Ku slave image shown in Figure 19 suffered significant blur causing large numbers of false alarms in the Ku CCD image. The actual target detections in blue are still easily observed.

Figures 18 and 19 help to illustrate the importance of viewing geometry and collection concept of operations (CONOPS). Except for very dense foliage, a target along a tree line or near a clump of trees is viewable from at least one direction. By properly planning the flight path and collection geometry, targets located within a right-of-way can readily be detected. In cases of dense foliage and for limited sections, collection along multiple flight paths may be needed.

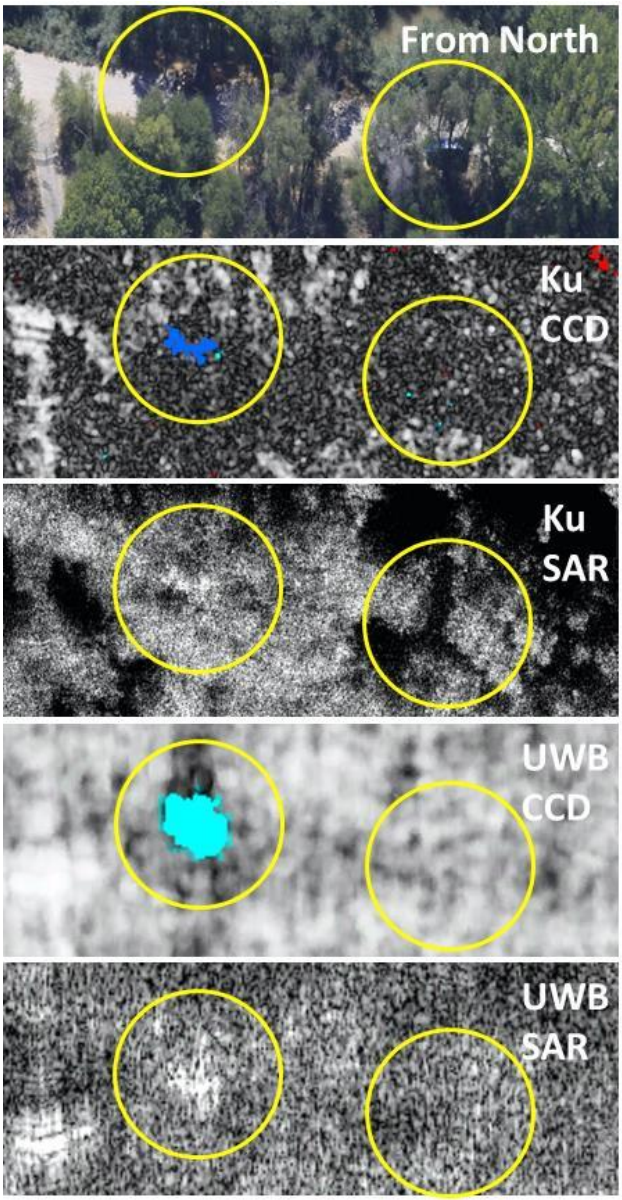

Figure 18. Backhoe and SUV in partially obscured locations. Backhoe is easily detected from open view point, while the SUV provided returns in the Ku data but they were small and not indicative of a vehicle. Only the backhoe was detected in the UWB data. SAR transmission is from the bottom facing up into the image.

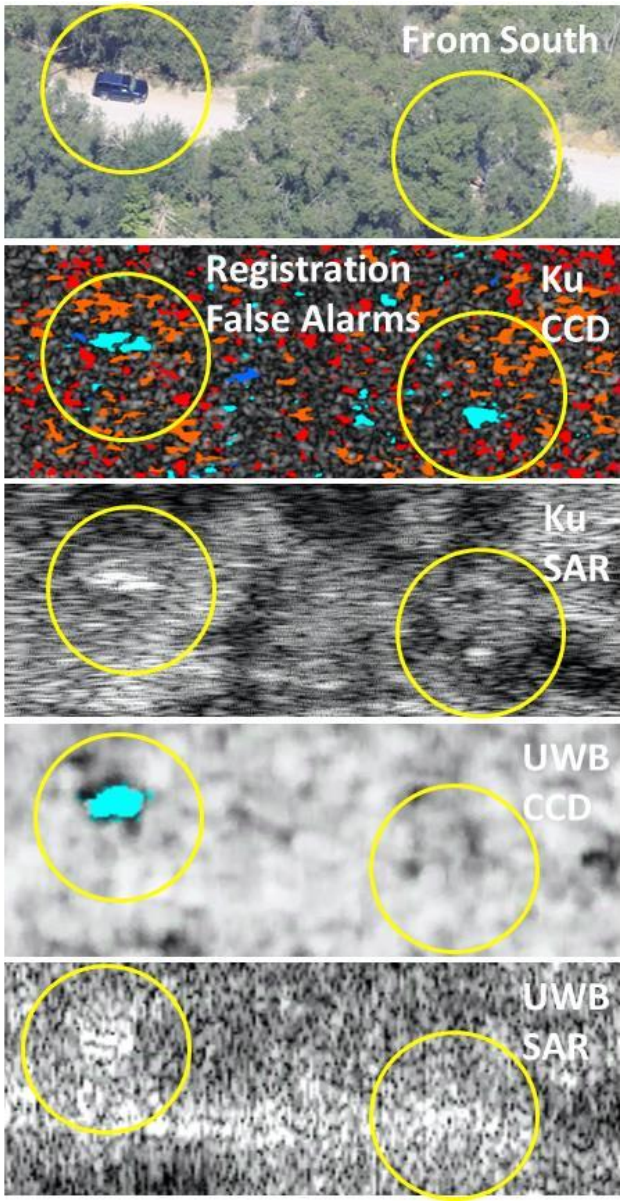

Figure 19. Backhoe and SUV viewed from opposite side. The un-obscured SUV is easily detected in both the Ku and UWB, while the mostly obscured backhoe is detected only in the Ku data. The Ku slave image suffered significant blur causing large numbers of false alarms as indicated in red. The actual target detections in blue are still easily observed.

Figure 20 shows a 24 August collection at the Provo Cemetery target site. In the images are three targets located in the open including a small pickup truck, a large corner reflector (3 ft) and a small corner reflector (1 ft). In the Ku data all three targets are easily detected. In the UWB data, only the pickup truck and large corner reflector are detected. The Provo cemetery location was the most industrial of the test locations and occasionally experienced some radio frequency interference (RFI) causing false alarms in the UWB results.

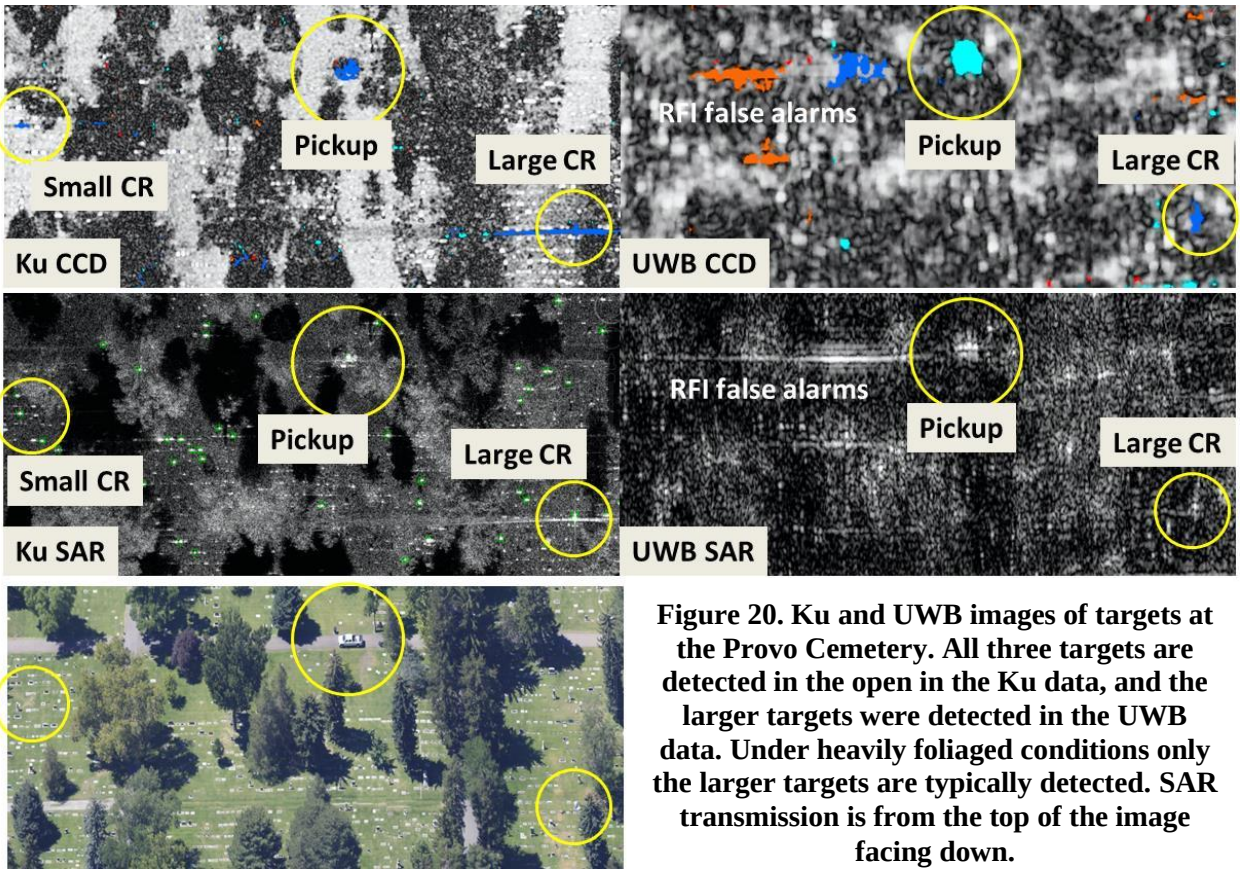

Figure 20. Ku and UWB images of targets at the Provo Cemetery. All three targets are detected in the open in the Ku data, and the larger targets were detected in the UWB data. Under heavily foliaged conditions only the larger targets are typically detected. SAR transmission is from the top of the image facing down.

For the PDPR program, over 3 terabytes of SAR data was collected and processed. Around 60% of the Ku data with targets and 30% of the UWB data with targets was manually reviewed to provide both qualitative and quantitative results. No X-band quantitative results are presented, but qualitatively, the X-band performed similarly to Ku for large targets.

Table 7 shows the 2017 quantitative Ku results separated by target size (large or small) and viewing status (open or covered/partially covered by vegetation). The same targets were not used at all testing sites and some sites were imaged more than others creating a variation in the total number of collects for each target type. Based upon Table 7, large targets are detected almost 100% of the time when located in an open viewing condition. Smaller targets were detected around 90% of the time when in the open. In covered or partially covered conditions, detection accuracies decrease to around 60% for large objects and less than 50% for small objects. As

detection depends on signal passage through gaps in the vegetation, smaller objects can be placed in deeper coverage, which limits their detection performance. The radar return strength or more formally called the radar cross section also impacts target detectability. Corner reflectors and targets with sharp corners like the backhoe provide stronger SAR returns. Objects with rounded and few corners provide weaker SAR returns. Table 8 shows the UWB quantitative detection results. Targets in the open showed similar performance to the Ku data and while targets in covered conditions showed more variation based on the type of target. The large detection performance difference between open and covered conditions illustrates how a collection CONOPS that optimizes collection from an open viewing geometry can increase the overall probability of detection.

Table 7. 2017 quantitative Ku results separated by target size (large or small) and viewing status (open or covered/partially covered by vegetation). Around 60% of the Ku data with targets was manually reviewed to generate these results.

Target	Size	Status	Return	No	Yes	Total	%No	%Yes
Backhoe	Large	Open	High	0	13	13	0%	100%
SUV	Large	Open	Medium	0	3	3	0%	100%
Pickup	Large	Open	Medium	0	7	7	0%	100%
Ranger	Large	Open	Medium	1	6	7	14%	86%
Large_CR	Large	Open	High	2	19	21	10%	90%
Small_CR	Small	Open	High	0	12	12	0%	100%
Wheelbarrow	Small	Open	Low	2	8	10	20%	80%
Backhoe	Large	Covered	High	7	10	17	41%	59%
SUV	Large	Covered	Medium	5	6	11	45%	55%
Pickup	Large	Covered	Medium	1	2	3	33%	67%
Ranger	Large	Covered	Medium	3	2	5	60%	40%
Large_CR	Large	Covered	High	4	9	13	31%	69%
Small_CR	Small	Covered	High	1	6	7	14%	86%
Wheelbarrow	Small	Covered	Low	15	2	17	88%	12%

Table 8. 2017 quantitative UWB 540 MHz results separated by target size (large or small) and viewing status (open or covered/partially covered by vegetation). Around 60% of the UWB data with targets was manually reviewed to generate these results.

Target	Size	Status	Return	No	Yes	Total	%No	%Yes
Backhoe	Large	Open	High	0	5	5	0%	100%
SUV	Large	Open	Medium	0	2	2	0%	100%
Pickup	Large	Open	Medium	1	6	7	14%	86%
Ranger	Large	Open	Medium	0	3	3	0%	100%
Large_CR	Large	Open	High	0	13	13	0%	100%
Small_CR	Small	Open	High	1	7	8	13%	88%
Wheelbarrow	Small	Open	Low	1	4	5	20%	80%
Backhoe	Large	Covered	High	1	10	11	9%	91%
SUV	Large	Covered	Medium	4	6	10	40%	60%
Pickup	Large	Covered	Medium	2	1	3	67%	33%
Ranger	Large	Covered	Medium	1	0	1	100%	0%
Large_CR	Large	Covered	High	2	3	5	40%	60%
Small_CR	Small	Covered	High	3	1	4	75%	25%
Wheelbarrow	Small	Covered	Low	9	1	10	90%	10%

A benefit of the higher resolution Ku SAR is the ability to detect past vehicle activity in the CCD image. Figure 21 shows a Ku CCD result from the Birdseye target area in which various levels of vehicle activity can be observed. As the optical image in Figure 21 shows, there are several dirt paths with a primary entrance from the highway road. The dark, low coherent, entrance area suggests that a few vehicles entered here and traveled along path 1. Similarly, vehicles traversed along path 3, with only limited use of paths 2 and 4. Path 4 is not visible in the EO image suggesting off-road vehicle activity. Other low coherence areas in Figure 21 are likely areas of wet soil.

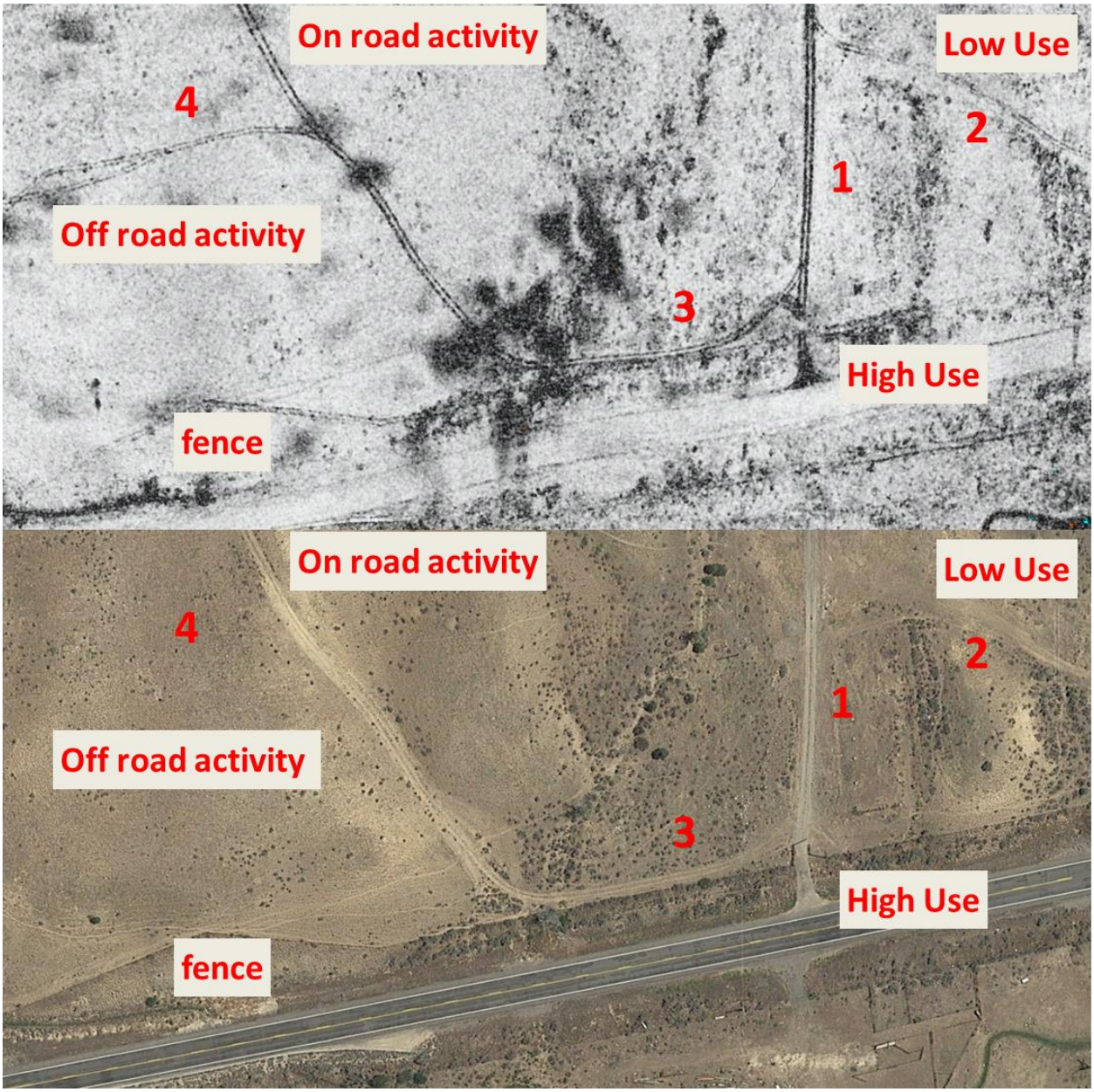

Figure 21. SAR CCD and associated EO image showing trails with various levels of on road and off road activity. SAR transmission is from the bottom facing up into the image.

Figure 22 shows the Ku detection results of the backhoe when positioned in two different orientations. Based on Figure 22, the orientation of large targets in the open can be determined from the CCD detection results. In contrast, the orientation of partially obscured targets is indeterminate due detection only through gaps in the foliage.

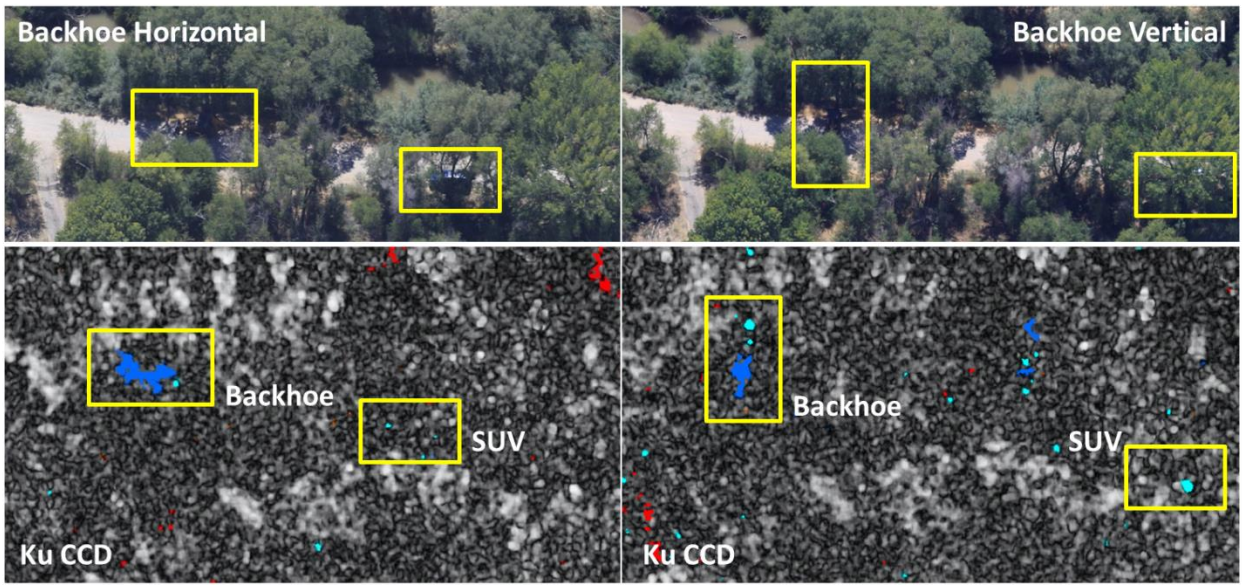

Figure 22. Ku detection helps the determination of object orientation for targets detected in the open. SAR transmission is from the bottom facing up into the image.

As mentioned previously, the full 540 MHz bandwidth approved for use by IMSAR in Utah was employed for the 2017 UWB collections. In actual operation, the approved bandwidth may be restricted as was anticipated for the Sacramento, CA collection. To simulate the impact of reduced bandwidth operation, UWB collections were reprocessed using the 210 MHz Sacramento frequency range. Figure 23 shows comparison UWB images using both the 540 and 210 MHz frequency ranges. From these images it is clear that the spatial resolution has decreased causing a bloating of objects in the scene. More importantly, the reduced resolution prevented the detection of the small wheel barrow in the 210 MHz data.

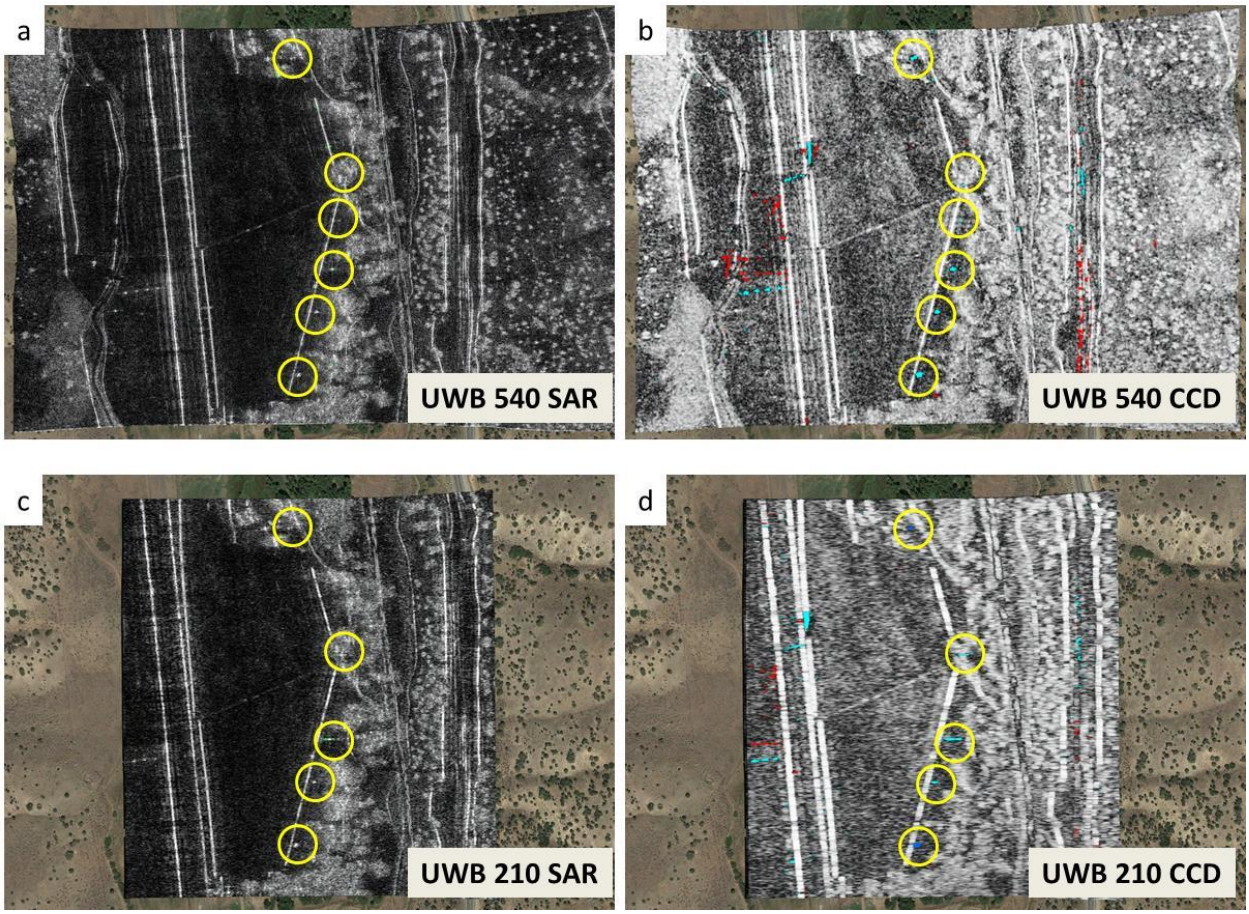

Figure 23. Bandwidth reduction increases the pixel size and prevented the detection of the wheel barrow target in the 210 MHz data. SAR transmission is from the left side of the image facing the right.

To better characterize the system in a more realistic operational scenario, "day-in-the-life" measurements were included in the July 2017 collections. For these collections a pipeline right-of-way along Payson Canyon was collected against on multiple days. Figure shows a context image and Ku CCD results after 1 day and after 2 days. No detections were found within the right-of-way area on either day. Looking at Figure 24, degradation in coherence is observable as a general darkening of the image. Additionally, localized areas of low coherence and large numbers of false alarms do to deviations in the flight plan from the baseline collection on day 0 are evident. Commercialization of this technology will require good CCD performance up to a week between collections, which will put additional constraints on the repeatability of the flight profiles.

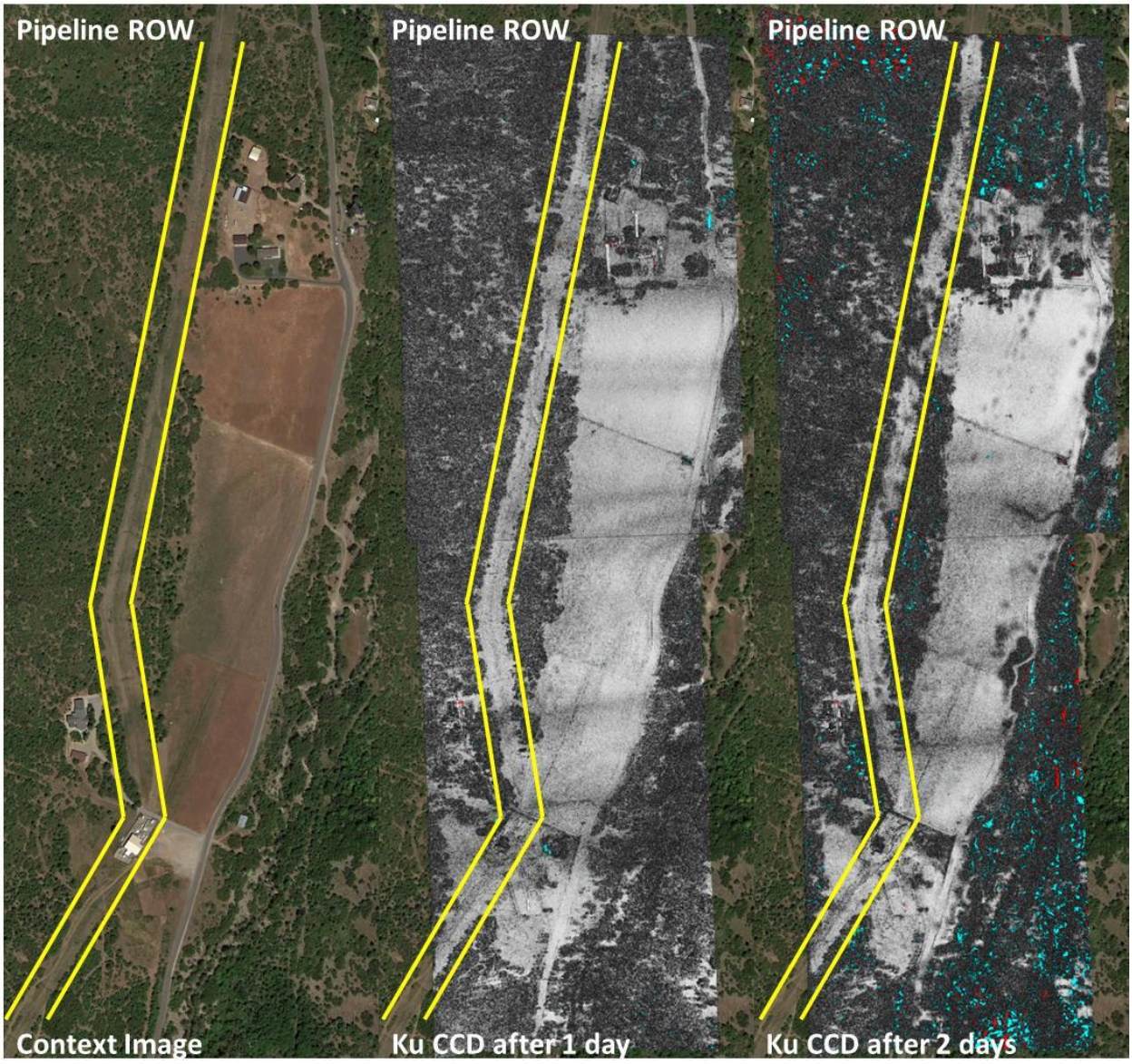

Figure 24. CCD images showing collection over a pipeline right-of-way area near Payson Canyon after 1 and 2 days. No detections were found within the right-of-way area. SAR transmission is from the right side of the image facing the left.

6 Summary

The emphasis of the PDPR project work thus far has been to characterize SAR performance under conditions specific to the identification of incursion threats on buried pipeline right-of-way covered by foliage. Three flight test campaigns have been completed enabling identification of enhancements then validation of multiple implemented SAR system hardware and software upgrades to improve performance specific to the pipeline operator's needs. Each flight test required considerable coordination between test coordinators, image analysts, test object stagers and flight crew enabling efficient execution of flight tests covering multiple surface

environments (i.e. urban and rural) and performance evaluation over three frequency bands. The ability to detect the presence of objects of a variety of sizes (i.e. from shovels to backhoes) within foliage covered and open viewing conditions was characterized. In addition, the testing evaluated the effectiveness of SAR change detection algorithms at revealing the movement of objects between successive overflights. Tests revealed that X and Ku band performances were comparable so, to simplify flight test logistics, we eliminated the X-band functionality from further consideration and limited the higher frequency focus solely to the more mature Ku-band system.

The Utah test results enabled us to quantify SAR performance as a function of object size and surface condition yielding an initial assessment of detection likelihood. It was not surprising that the shovel could not be detected, or that the likelihood of detection for the remaining objects increased with object size (i.e. increasing radar cross section). The test results also confirmed our expectations for detection of objects obscured by foliage. In this case, the likelihood of detection decreased for all object types when compared to the open environment. Due to the longer wavelengths, the UWB signal is more likely to penetrate the canopy albeit with reduced resolution (i.e. lower transmit signal bandwidth) when compared to Ku-band. However, while the wider Ku-band transmit signal improved ground resolution, the shorter transmit wavelengths were less likely to penetrate the foliage canopy. At Ku-band, detection of objects obscured by canopy is largely determined by the extent of foliage coverage i.e. detection probability increases if there are openings in the canopy enabling the radar signal to reach the object without interference. The change detection algorithm effectiveness was confirmed as well. The UWB system was more likely to detect change beneath canopy than Ku-band, but with reduced resolution while the Ku-band system produced higher resolution results in open areas and was unreliable for objects beneath canopy.

The tests also revealed several hardware and software enhancements that were integrated into the SAR systems during the course of the project. While these upgrades have produced considerable performance improvement, additional changes are needed to reduce the rate of false detections to an acceptable level required prior to any commercial deployment.

At this point the emphasis of the project will shift from performance characterization and stabilization to engagement with prospective pipeline operators to assess their specific operational needs and integrate this information into the commercialization plan. Commercialization of SAR for pipeline damage threat prevention will require additional hardware and software enhancements to address observed data anomalies. Anomalies, such as those shown in Figures 25 and 26, experienced during flight testing resulted from INS and radar data loss associated with data compression processing or the transmission of compressed data to the ground. Reprocessing from the original data file and software checks to identify corrupted images will correct most of these types of errors. Other errors, such as tree parallax and low coherence (Figure 27), result from differences in the flight profiles between the master and slave

images. IMSAR's flight support software provides guidance to the pilot on the flight profile. Improvements in flight planning to ensure straighter flight paths along with the addition of a line-of-sight velocity indicator for the pilot will mitigate this anomaly in future collections. Other anomalies such as mis-registration can be mitigated through software checks and automated reprocessing based on the number of CCD detections. Advanced deep machine learning models could also be implemented to aid in rejection of false detections due to mis-registration error.

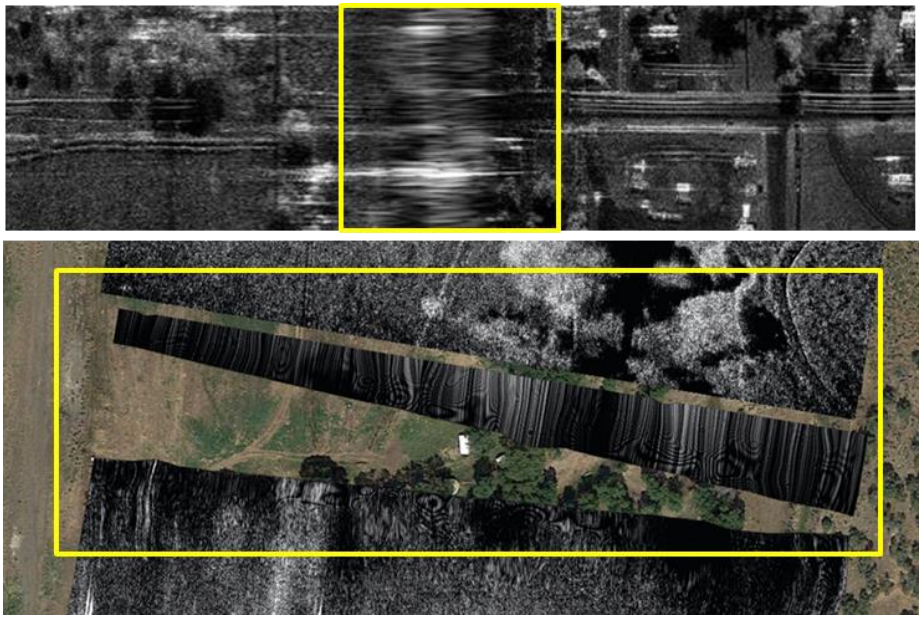

Figure 25. Data anomalies caused by transmission errors from the plane to the ground downlink site. Reprocessing of the raw data can recover the corrupted results.

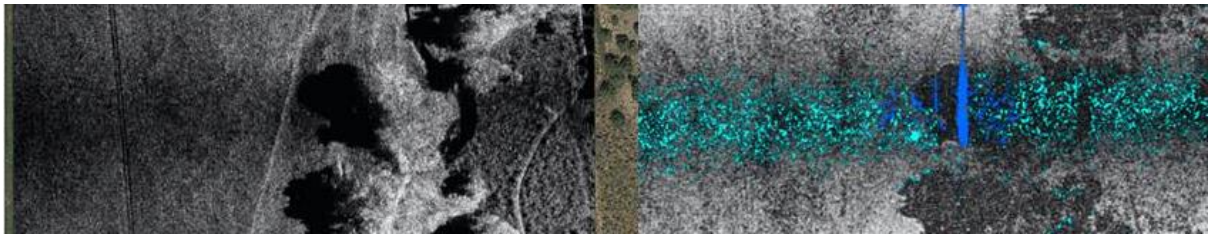

Figure 26. Area of low coherence caused by the loss of radar information during data compression. Updates to the compression software will prevent this anomaly in the future.

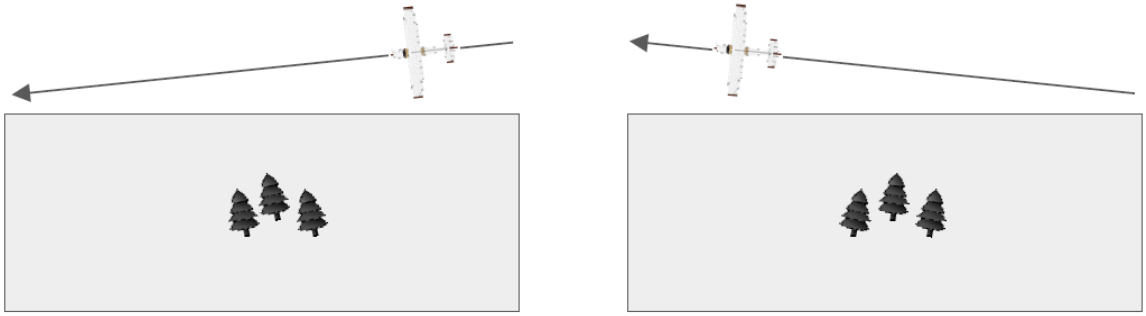

Figure 27. Variances in collection flight paths can induce parallax in taller objects and low coherence CCD results.

7 Impact from Research Results

The research completed under the PDPR project enabled optimization and performance validation of airborne SAR technology specifically for application to vehicle and object identification on buried pipeline right-of-way (ROW) obscured by foliage. Several radar system hardware, software and image processing modifications were identified, developed, implemented and verified during the course of this project. The following subsections highlight the modifications that produced the greatest improvements and describe their importance to the foliage penetration objective.

7.1 Dual Band Operation

Collecting SAR data over multiple frequency bands provides an independent look of the scene in processed imagery which improves the probability of detection of objects hidden from view by foliage. During the field campaign we evaluated the PDPR's performance in the UWB, X and Ku frequency bands. The UWB band operates with the longest wavelength and is impacted the least by signal attenuation through foliage. However, the relatively narrow transmission bandwidth approved for use by the FCC limits spatial resolution of the imagery. Conversely, while wider transmission bandwidths (and finer resolutions) are available in the higher two frequency bands, their signals experience far greater attenuation through foliage. While signals at these frequencies are unable to "see through" dense foliage, they can provide a valuable higher resolution perspective of the ground scene when there are openings in the canopy. Following analysis of field test results we selected the high-resolution performance of the Ku-band to complement the foliage penetration performance of the UWB. We found that while the foliage penetration capability of the Ku band was very limited and comparable to X-band, the resolution and sensitivity to surface change improved. The ability to detect vehicles through canopy openings with higher resolution and to detect surface changes caused by prior vehicular movement disturbing soil is an important additional tool that operators can use for pipeline area monitoring.

7.2 Antenna Array

A 3-element LP antenna array configuration was incorporated into the UWB system for the 2017 tests to help reject RFI, improve SNR and reduce the ghosting/scratching/blurring observed in images during the June 2016 collections. The June 2016 tests were performed using only a single LP antenna element. Since the power received by the radar is directly proportional to the antenna gain-squared (a factor of 2X in dB), the antenna gain increase (ideally nearly 5 dB) of the 3-element LP antenna can produce a received power increase of nearly 10 dB (i.e. 10X) over the single antenna element design. The gain increase improves the radar's foliage penetration capability (with no increase in transmit power) and detection probability, and also increases SNR making the received signal more resistant to noise and interference.

7.3 Co-Boresighted, High Resolution Camera

Co-boresighted and co-registered high resolution optical imagery is a critical component of pipeline monitoring and complements aerial radar observation by providing context imagery to support SAR analysis and the generation of data products. The 2016 field test campaign relied upon a 5 Mpixel camera for optical imagery that was not co-boresighted with the radar antennas. While this capability was sufficient at the time to complete radar performance evaluations, it would not suffice in an operational environment. A key improvement implemented for the 2017 data collections was the addition of an 18 Mpixel gimbaled and co-boresighted optical camera. The 3.6X improvement in ground resolution provides critical optical clarity that is more easily interpreted enabling operators to identify specific ground features and objects that were cued by SAR reports (e.g. vehicle detections or surface changes) and to determine the best course of action. The addition of high resolution optical imagery expands the PDPR capability beyond just SAR and into a true multi-spectral capability.

7.4 Image Registration

The 2016 testing revealed errors in the position data reported by the INS causing image blurring and registration errors between the baseline (master) and slave images. Registration error causes an offset between consecutive SAR images of the same scene reducing coherence and producing an increase in false positive detections following change detection processing. A software upgrade for INS signal filtering and noise reduction was designed and installed to mitigate this effect. Flight tests confirmed the performance improvement.

7.5 Change Detection

The project's primary objective was to optimize the airborne SAR system for detection of excavation equipment operating on buried pipeline ROW that is obscured from view by brush and forest canopy. Since the baseline operational approach requires periodic retracing of flight paths that run parallel to the ROW, we're also able to use SAR image data collected from consecutive flights to detect surface change in addition to actual vehicles. This surface change measurement capability is a valuable supplement to the baseline detection capability. Since the likelihood of vehicle detection is directly proportional to the frequency of overflights (i.e. time

over the ROW area) it's highly likely that there could be considerable time between aerial observations. Unauthorized excavation could be occurring during these extended unobserved time intervals and may only be detectable using SAR change detection techniques.

Change is quantified in SAR images by measuring the difference (in magnitude or phase) pixel by pixel between two co-registered images obtained over the same area at different times. A change is identified by a decrease in coherence which is highlighted by the change detection (CD) process. The SAR image areas containing change can then be superimposed onto optical imagery for geographical context. CD can reveal vehicle movement into or out of ROW areas and is typically depicted using red to indicate object movement out of an area or blue for movement into an area, ("red fled" or "blue new" using the DoD vernacular). Detection of ground surface change caused by vehicle movement disturbing soil (i.e. tire tracks and excavation) can be measured in areas not obscured by foliage.

We evaluated the performance of both magnitude and coherent change detection (MCD and CCD, respectively) methods in the UWB and Ku frequency bands during the flight tests. CCD implies phase measurement and is more sensitive than the MCD method but is also more susceptible to image registration, flight track retrace consistency, aircraft attitude and instrument measurement errors. There errors can induce false change results. The MCD method is dependent upon amplitude change, is less susceptible to error and produces fewer false detections. The change measurements depicted earlier in this report used the MCD method. As mentioned earlier, foliage penetration performance is best using the lower frequency UWB radar. Over open areas, the Ku-band radar is more sensitive to change and provides higher spatial resolution. The combination of these two bands is optimal for vehicle detection and surface change detection measurement and provides the pipeline operator with a valuable supplemental measurement enabling assessment of ROW changes occurring between aerial patrols.

7.6 Collection Planning and Execution

This research demonstrated that the most effective way to detect objects in ROW areas is to collect under open conditions. The large detection performance difference between open and covered conditions illustrates how flight planning that optimizes collection from an open viewing geometry increases the overall probability of detection. Likewise, increasing SAR penetration performance and detection likelihood through foliage and dense vegetation may require image collection from both sides of the ROW.

8 Business Status

All tasks and milestones have been completed for the PDPR project except for "present paper at public event/forum," which is planned for April, 2018. The final billable milestones completed in this final quarter includes this Final Report, the public version of the final report, and the Commercialization Plan. There was no cost sharing during this quarter and all cost sharing has been realized.

9 Payable Milestones

The payment milestones completed this quarter and are summarized in Table 9.

Table 9. Status of the Payment Milestones for Quarter 4, 2017 of the PDPR project.

Milestone	Status
Final Report	Completed
Public Version of Final Report	Completed
Commercialization Plan	Completed